

CRITICAL ANALYSIS OF ANTIBODY CATALYSIS

Donald Hilvert

*Laboratorium für Organische Chemie, Swiss Federal Institute of Technology (ETH),
Universitätstrasse 16, 8092 Zurich, Switzerland; e-mail: hilvert@org.chem.ethz.ch*

Key Words antibody, enzyme, transition-state analog, mechanism of catalysis, catalytic efficiency

■ **Abstract** Antibody molecules elicited with rationally designed transition-state analogs catalyze numerous reactions, including many that cannot be achieved by standard chemical methods. Although relatively primitive when compared with natural enzymes, these catalysts are valuable tools for probing the origins and evolution of biological catalysis. Mechanistic and structural analyses of representative antibody catalysts, generated with a variety of strategies for several different reaction types, suggest that their modest efficiency is a consequence of imperfect hapten design and indirect selection. Development of improved transition-state analogs, refinements in immunization and screening protocols, and elaboration of general strategies for augmenting the efficiency of first-generation catalytic antibodies are identified as evident, but difficult, challenges for this field. Rising to these challenges and more successfully integrating programmable design with the selective forces of biology will enhance our understanding of enzymatic catalysis. Further, it should yield useful protein catalysts for an enhanced range of practical applications in chemistry and biology.

CONTENTS

EXPLOITING ANTIBODIES AS CATALYSTS	752
CATALYTIC EFFICIENCY	752
HAPTEN DESIGN	754
REPRESENTATIVE CATALYTIC ANTIBODIES	755
Proximity Effects	755
Strain	766
Electrostatic Catalysis	769
Functional Groups	776
PERSPECTIVES	781
General Lessons from Comparisons of Enzymes and Antibodies	781
How Efficient Does Catalysis Need to Be?	782
Strategies for Optimizing Efficiency	783
CONCLUSIONS	787

EXPLOITING ANTIBODIES AS CATALYSTS

Some three decades ago, Jencks suggested that stable molecules resembling the transition state of a reaction might be used as haptens to elicit antibodies with tailored catalytic activities and selectivities (1). Implementation of this clever idea was made possible by the development of monoclonal antibodies, viable transition-state analogs, and versatile screening assays, and more than 100 reactions have now been successfully accelerated by antibodies (2, 3). These include pericyclic processes, group transfer reactions, additions and eliminations, oxidations and reductions, aldol condensations, and miscellaneous cofactor-dependent transformations. Because selectivities in these systems generally reflect the structure of the hapten and can rival those of natural enzymes, transformations that cannot be achieved efficiently or selectively via more traditional chemical methods are the subject of much current research (4).

Total synthesis of the natural product epothilone from a chiral intermediate prepared by antibody catalysis (5) and activation of a prodrug *in vivo* (6) are two recent accomplishments that illustrate the potential of this technology. Nevertheless, practical applications are still the exception rather than the rule. Low catalytic efficiency, in particular, appears to be a significant limitation. While modest rate accelerations are easily achieved, enzymelike activity remains elusive. The goal of this review is to address this problem in light of recent structural and mechanistic work. After first considering the intertwined issues of catalytic efficiency and hapten design, a few well-characterized examples of antibodies promoting a diverse set of reactions are used to illustrate how antibody binding energy is exploited for catalysis and to identify factors that limit overall efficiency. Finally, possible strategies for improving these systems are discussed.

CATALYTIC EFFICIENCY

By almost any criterion, natural enzymes are incredibly efficient catalysts. The fastest enzymes are limited by the rate at which they encounter substrate, and even those that have not achieved this level of evolutionary perfection typically have apparent bimolecular rate constants ($k_{\text{cat}}/K_{\text{m}}$) between 10^6 and $10^8 \text{ M}^{-1} \text{ s}^{-1}$, irrespective of the rate of the corresponding uncatalyzed reaction (7). Rate accelerations over background ($k_{\text{cat}}/k_{\text{non}}$) are also very high, in the range of 10^6 to 10^{12} , and can even reach 10^{17} in some special cases (7, 8).

These extraordinary effects have been explained by the ability of an enzyme to bind transition states more tightly than ground states (9). When enzymatic and nonenzymatic reactions occur by the same mechanism and chemistry is rate determining, a simple thermodynamic cycle based on transition-state theory can be used to show that $k_{\text{cat}}/k_{\text{uncat}} = K_{\text{m}}/K_{\text{TS}}$, where K_{m} and K_{TS} are the dissociation constants for substrate and transition state from the enzyme (10, 11). The chemical proficiency of an enzyme, as defined by Wolfenden (7), is then given as the ratio

$(k_{\text{cat}}/K_{\text{m}})/k_{\text{uncat}}$ or $1/K_{\text{TS}}$. This term represents the lower limit of the affinity of a protein for the transition state and varies from 10^8 to 10^{23} M^{-1} for a series of natural enzymes (7, 8). Although true transition-state affinity may be underestimated if chemistry is not cleanly rate limiting or if the enzyme uses a different mechanism than the uncatalyzed reaction, this term provides a useful measure of catalytic power for the purpose of discussion.

One practical consequence of the application of transition-state theory to enzymes has been the design of potent inhibitor molecules through mimicry of structural and electronic features of otherwise ephemeral transition states (for recent reviews, see 12–14). Another has been the use of such compounds to generate catalytic antibodies (2, 3). The latter strategy has been found to be broadly useful, as any chemical transformation compatible with a biological milieu is potentially amenable to antibody catalysis so long as an appropriate transition-state analog can be devised.

Broad scope and high, programmable catalyst selectivity certainly make this route to tailored enzymes one of the most promising to emerge in the last two decades. In terms of efficiency, however, catalytic antibodies do not yet match their natural counterparts. Published $k_{\text{cat}}/K_{\text{m}}$ values for the best catalysts are only in the range of 10^2 to $10^4 \text{ M}^{-1} \text{ s}^{-1}$, well below the limit for diffusion-controlled processes, and rate accelerations are usually between 10^3 - and 10^5 -fold over background (15, 16). Smaller effects are often found, but higher efficiencies are extremely rare.

Differences between antibodies and enzymes are readily apparent in Figure 1, where rate acceleration is plotted against chemical proficiency for a representative set of reactions. Antibody-catalyzed reactions cluster in the lower left quadrant of the plot, corresponding to the lowest activities, whereas enzymatic reactions lie above and to the right, spanning a much greater range of efficiency. Because K_{m} values are roughly comparable in all of these systems, an excellent correlation between rate acceleration and proficiency is observed. In essence, better transition-state binding translates directly into higher activity. Although the best antibodies approach the efficiency of the least efficient enzymes, it should be noted that the corresponding reactions often involve conversions of relatively activated substrates (e.g. the hydrolysis of aryl esters). In contrast, enzymes specialize in accelerating extremely slow reactions like the cleavage of amides (with a half-life, $t_{1/2}$, for the uncatalyzed reaction of 7.3 years) and phosphate diesters ($t_{1/2} = 130,000$ years), few of which have yielded to significant antibody catalysis.

In a complementary analysis, Stewart & Benkovic (15) found a weak correlation between rate acceleration and the ratio of the equilibrium binding constants of the reaction substrate and the hapten: $k_{\text{cat}}/k_{\text{non}} = K_{\text{m}}/K_{\text{TS}} \approx K_{\text{m}}/K_{\text{i}}$. In other words, affinity for the transition-state analog roughly approximates affinity for the true transition state, in accord with the basic premise underlying the production of catalytic antibodies. Practically speaking, this means that the search for high-performance catalysts can often be reduced to a search for the best hapten binders—provided the hapten is a reasonably good transition-state mimic. However, association constants for low-molecular-weight haptens ($1/K_{\text{i}} = 10^6$ – 10^{10} M^{-1}) are

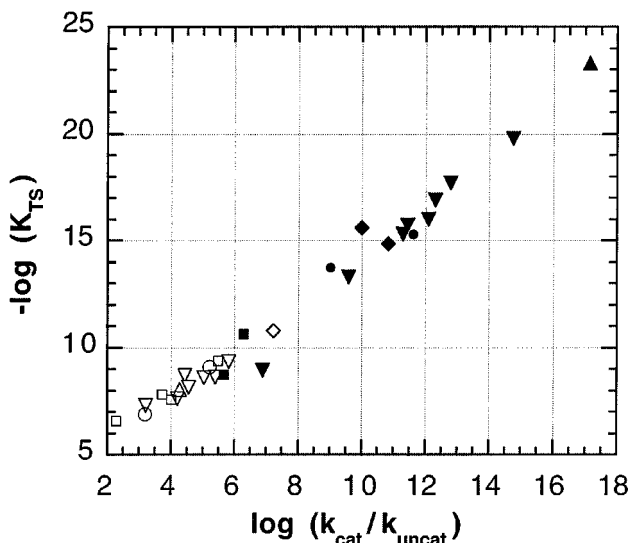


Figure 1 Comparison of chemical proficiency, $-\log(K_{TS})$, and rate acceleration, k_{cat}/k_{uncat} , for a series of reactions catalyzed by enzymes (filled symbols) and antibodies (open symbols). Rearrangements (\blacksquare , \square), hydrolyses (\blacktriangledown , \triangledown), decarboxylations (\blacktriangle , \bullet), deprotonations (\bullet , \circ), and retroaldol reactions (\blacklozenge , \diamond) are included. (Enzyme data are from References 7, 112, 131, 132, and antibody data are from References 25, 26, 38, 75, 91, 110, 113, 115, 121, 127, 200–202.)

generally much smaller than chemical proficiencies of the most effective enzymes. Given K_m values of $\sim 10^{-4}$ M, these affinities suggest that k_{cat}/k_{uncat} will seldom exceed $\sim 10^6$ for first-generation catalytic antibodies, as found experimentally. For reactions with modest activation barriers, effects of this magnitude may be useful. If product inhibition and protein production pose no further technical hurdles, kinetic resolutions can be achieved, the fate of reactive intermediates controlled, and so on. For truly difficult reactions, however, such effects are almost certainly inadequate.

HAPTEN DESIGN

Before turning to a description of specific antibodies, a few words about hapten design are in order. Transition states themselves have fleeting lifetimes and cannot be isolated. Synthesis of effective analogs must therefore draw on our chemical intuition about the conformational, stereochemical, and electronic properties of the reaction under study. Because no stable molecule can reproduce all characteristics of an actual transition state, design efforts have tended to focus on salient features

distinguishing transition state from ground state (12–14). For instance, changes in hybridization or charge occurring as a reaction proceeds can be mimicked by incorporating different elements or charged groups at appropriate sites within the analog. Conformational constraint can help approximate the reactive geometry of a flexible substrate, while multisubstrate analogs may be used to imitate the relative disposition of reactants in a bimolecular process.

For reactions that require catalytic functionality within the antibody pocket, more sophisticated strategies appear to be needed. In the bait-and-switch approach, charge complementarity between hapten and antibody is exploited to induce appropriately positioned acids, bases, and nucleophiles. Alternatively, catalytic residues can be selected directly by irreversible chemical modification when mechanism-based inhibitors (17, 18) are employed as haptens. The latter strategy, dubbed reactive immunization (19), has the virtue of allowing rational engineering of covalent catalysis.

For each new reaction, hapten design must be optimized to maximize the probability of finding an antibody catalyst. Because subtle differences between even the best transition-state analogs and actual transition states almost certainly contribute to lower efficiencies of antibodies compared with enzymes, it is important to understand how instructions implicit in any given hapten design are realized in the complementary immunoglobulin binding pocket. Characterization of successful antibody catalysts at the atomic level currently provides the most useful insights into how binding energy is exploited for catalysis.

REPRESENTATIVE CATALYTIC ANTIBODIES

Proximity Effects

Utilization of binding energy to constrain flexible molecules into reactive conformations or to preorganize reactants for bimolecular reaction is a potentially powerful strategy for accelerating reactions with unfavorable entropies of activation (20, 21). To test whether antibodies might serve as entropy traps (21), concerted pericyclic reactions requiring neither nucleophilic nor acid-base catalysis have been investigated.

Sigmatropic Rearrangements The biologically important Claisen rearrangement of chorismate to prephenate (Figure 2) and the abiological oxy-Cope rearrangement (Figure 3) are typical [3,3]-sigmatropic processes. They proceed via highly ordered, entropically unfavorable, cyclic transition states involving simultaneous formation of a carbon-carbon bond and cleavage of either a carbon-oxygen or another carbon-carbon bond.

For the chorismate rearrangement, the conformationally locked oxabicyclic dicarboxylic acid (labeled **1** in Figure 2) (22) proved to be a successful hapten. It

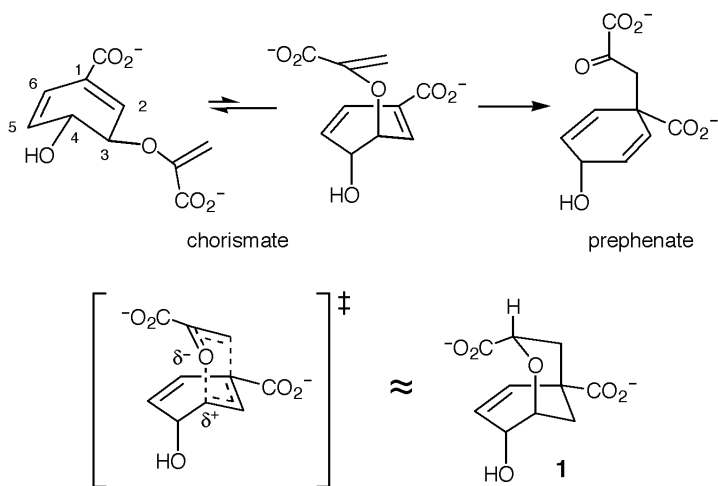


Figure 2 (Top) The Claisen rearrangement of chorismate to prephenate catalyzed by antibody 1F7; the flexible chorismate adopts an extended pseudo-diequatorial conformation in solution and must undergo a conformational change to populate the less stable pseudo-diaxial conformer in order for the reaction to proceed. (Bottom) The conformationally restricted dicarboxylic acid **1** (22) mimics the transition state of the Claisen rearrangement and was used to elicit catalytic antibody 1F7 (25).

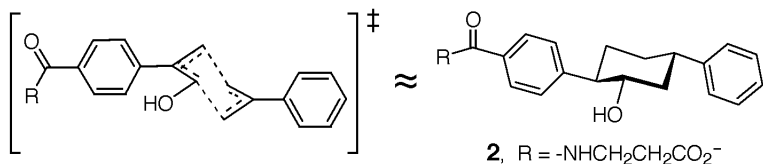
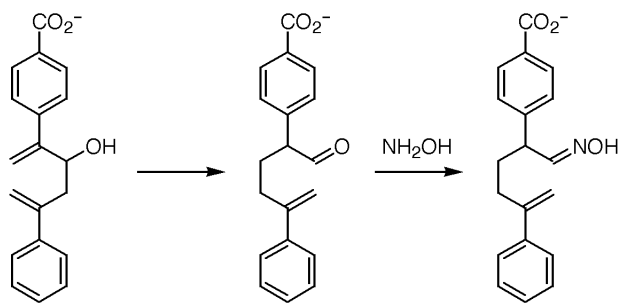


Figure 3 Antibody-catalyzed oxy-Cope rearrangement (36). The aldehyde product is trapped with hydroxylamine to give an oxime to prevent time-dependent inactivation of the catalyst. The 2,5-diaryl cyclohexanol derivative **2** was used to imitate the structure of the pericyclic transition state.

has a chairlike geometry very similar to that of the presumed transition state and is an effective inhibitor of natural chorismate mutases ($K_i = 0.12$ to $3 \mu\text{M}$) (22, 23). Antibodies that bind **1** catalyze the chorismate rearrangement enantioselectively with rate accelerations ($k_{\text{cat}}/k_{\text{uncat}}$) of 10^2 to 10^4 over background (24–27). For comparison, enzymes accelerate this reaction by a factor of $\sim 10^6$ (28). Spectroscopic and X-ray studies of 1F7 (which achieves a 200-fold rate enhancement) have provided insights into the origins of catalysis in these systems.

Transferred nuclear Overhauser effects (TRNOEs) show that 1F7 binds the flexible chorismate molecule in the diaxial conformation specified by the transition-state analog (29). Crystallographic data confirm that the induced binding pocket faithfully reflects hapten design (30). Compound **1** is deeply buried in the complex, and the overall shape and charge of the active site are complementary to a single hapten enantiomer (Figure 4a). Consequently, only the corresponding (–)-isomer of chorismate binds in a conformation appropriate for reaction. The subsequent rearrangement of bound substrate then occurs by the same concerted mechanism as that deduced for the uncatalyzed reaction and for natural chorismate mutases.

Nevertheless, 1F7 is likely to be a much poorer entropy trap than mutase enzymes. It exploits many fewer hydrogen bonds and electrostatic interactions for ligand recognition (Figures 4a, b). It also appears to accommodate charge separation in the transition state less effectively. Isotope effects show that the transition state for the rearrangement is highly polarized, with C–O bond cleavage preceding C–C bond formation (31, 32). As a consequence, the ether oxygen of the breaking C–O bond is partially negatively charged. The enzymes stabilize this species electrostatically by placing a cationic residue (either Arg or Lys) nearby (28, 33, 34), but 1F7 lacks an analogous feature (Figure 4a, b). These differences presumably explain the 10^4 -fold lower efficiency of the antibody. They can be attributed, in large part, to shortcomings in hapten design. While **1** reproduces the geometry of the actual transition state reasonably well, it mimics the polarized character of this high-energy species poorly (35).

Shortcomings in hapten design are also likely to account for the modest activity of antibody AZ-28. This antibody was raised against cyclohexanol derivative **2** ($K_d = 17 \text{ nM}$) and catalyzes the oxy-Cope rearrangement of the corresponding 2,5-diaryl-3-hydroxy-1,5-hexadiene with a $k_{\text{cat}}/k_{\text{uncat}}$ of 5300 (Figure 3) (36). In this case, disposition of the aryl substituents in the transition state is imitated imperfectly in the stable hapten.

Like the chorismate mutase antibody, AZ-28 has been shown by TRNOE measurements to preorganize the normally extended hexadiene substrate into a cyclic conformation so that its termini are in close proximity (37). In this case, ligand recognition is mediated by extensive van der Waals contacts, π -stacking interactions with the aromatic rings, and hydrogen bonding interactions with the alcohol, all evident in the X-ray structure of the antibody-hapten complex (Figure 5) (38). However, the conformation adopted by the substrate at the AZ-28 active site is

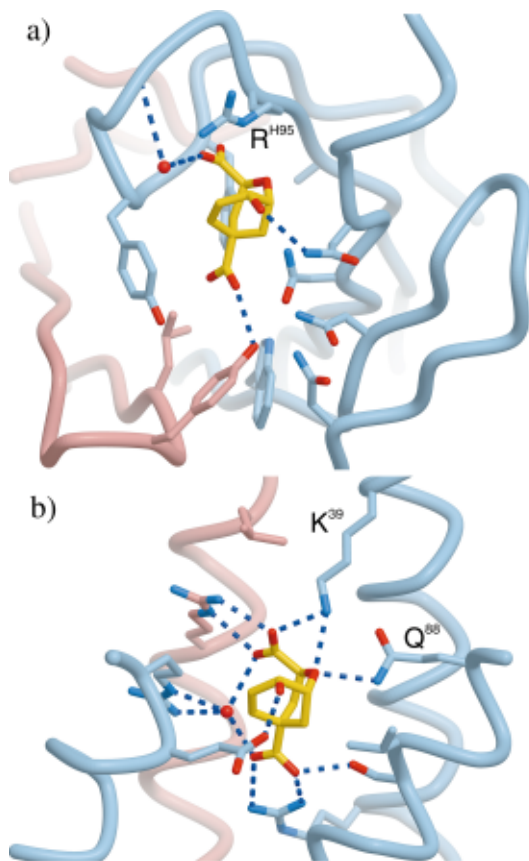


Figure 4 (a) Active site of antibody 1F7 (30), showing interactions with hapten **1** (see Figure 2). The light and heavy chains are *pink* and *blue*, respectively; the hapten is *yellow*. Note that Arg^{H95} forms a salt bridge with the secondary carboxylate of the ligand but is too far to form a hydrogen bond with the ether oxygen of **1**. (b) Active site of *E. coli* chorismate mutase (203). Bound **1** is completely inaccessible to solvent and makes numerous contacts with protein residues; hydrogen bonds from Lys³⁹ and Gln⁸⁸ to the ether oxygen of the ligand are essential for high activity (28). Graphics were prepared with the programs BobScript (204) and Raster3D (205).

unlikely to be optimal for reaction. The two aryl substituents at C-2 and C-5 are key recognition elements (Figure 5) but are oriented very differently in the hapten, where they are sp³ hybridized and equatorial to the plane of the cyclohexane ring, and the transition state, where they are sp² hybridized and conjugated with the reacting olefins (Figure 3). Thus, even though the hapten-induced pocket brings together the ends of the hexadiene substrate, binding energy directed to the peripheral aryl groups almost certainly imposes physical constraints that preclude

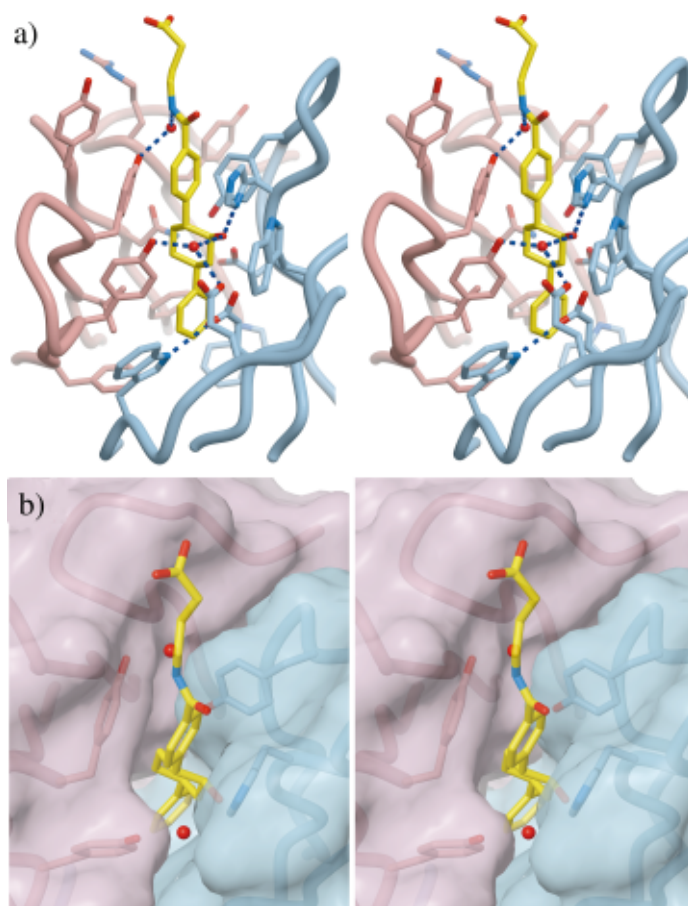


Figure 5 (a) Stereoview of the AZ-28 active site showing hapten-contacting residues (38). The 5-phenyl ring of **2** sits deep in the hydrophobic pocket, while the 2-phenyl substituent and linker are near the surface. The alcohol of the hapten forms a hydrogen bond with His^{H96}. Two water molecules in the pocket are depicted as *red spheres*. (b) GRASP (206) surface representation of AZ-28 showing the high degree of shape complementarity between ligand and protein.

effective alignment of the reacting $[4\pi + 2\sigma]$ orbitals. Alterations in antibody structure leading to improved orbital overlap should therefore result in significant increases in catalytic efficiency.

This inference is supported by studies of the germ line precursor of AZ-28. This antibody binds hapten **2** with 40-fold lower affinity than the mature AZ-28 but it is a substantially better catalyst, achieving a 163,000-fold rate acceleration over background (38). Mutagenesis experiments showed that replacement of Ser^{L34} in

the germ line sequence with Asn is responsible for both effects (38). In the crystal structure of AZ-28 (Figure 5), Asn^{L34} interacts directly with the cyclohexyl ring of the hapten and is therefore in a position to influence the conformation of the substrate at the active site.

Although designed as entropy traps, and despite evident restriction in the conformational freedom of their substrates, neither 1F7 nor AZ-28 lowers the entropy of activation (ΔS^\ddagger) for its reaction. Both have ΔS^\ddagger values that are 10–20 cal K⁻¹ mol⁻¹ less favorable than the corresponding uncatalyzed reaction (25, 37). This contrasts with some natural chorismate mutases that do reduce the entropy barrier significantly (39). Mechanistic interpretations of activation parameters are necessarily uncertain (40), but the unfavorable ΔS^\ddagger values are consistent with the need for substantial conformational change in the bound substrate as the reaction proceeds. However, other factors, including changes in solvation or conformation associated with the antibody, cannot be excluded.

More generally, these two examples show how the chemical instructions implicit in hapten structure, including deficiencies with respect to transition-state mimicry, are accurately imprinted on an antibody binding site. Improved transition-state analogs should therefore yield much better catalysts. To obtain more efficient chorismate mutase antibodies, for example, haptens containing additional negative charges might be used to elicit the catalytically essential cation in the vicinity of the ether oxygen of the substrate. Similarly, haptens in which the aryl substituents are coplanar with the cyclohexyl ring should increase the probability of identifying faster catalysts for the oxy-Cope rearrangement of Figure 3. The sensitivity of the latter reaction to anionic substituent effects (41) could also be drawn on. Haptens containing an appropriately positioned ammonium group might induce an antibody residue capable of deprotonating the substrate alcohol.

Fine-tuning of the first-generation antibodies is also likely to yield substantially better catalysts. Identification of a second chorismate mutase antibody possessing significantly higher activity than 1F7 (26) supports the feasibility of such an undertaking. Plausible strategies for optimizing activity include site-directed mutagenesis or random mutagenesis coupled with *in vivo* selection. The ability of the 1F7 Fab fragment to replace the missing enzyme in chorismate mutase-deficient yeast cells (42) is a promising indication that it will be amenable to directed evolution in the laboratory (43).

Overall, there are many ways to bind any given transition-state analog, only some of which will be effective for catalysis. Indeed, a significant fraction of hapten binders in any given experiment is usually found to be inactive. Hapten affinity rather than catalytic activity drives maturation of the immune response, so mutations can arise that favor tighter hapten binding but are deleterious for catalysis, as seen for AZ-28. Broad screening of antibodies raised to each hapten is therefore necessary to guarantee a representative sampling of the immune response. In the present instance, antibodies other than 1F7 and AZ-28 might be obtained that ultimately prove to be better starting points for optimization.

Cycloadditions Loss of both translational and rotational degrees of freedom should make bimolecular reactions particularly sensitive to proximity effects (20). Diels-Alder reactions between dienes and dienophiles have been used to test this notion. They typically have high activation entropies in the range of -30 to -40 cal K^{-1} mol^{-1} (44), reflecting the low probability of bringing together two substrates in an orientation optimal for reaction. The transition state for these concerted cycloadditions is highly ordered and resembles the boat form of the cyclohexene product more closely than it does the starting materials. Antibodies raised against bicyclic compounds that mimic the transition-state geometry have displayed a range of useful catalytic effects, including control over reaction pathway and absolute stereochemistry (45–49).

The general approach to catalysis is exemplified by antibody 1E9, which promotes the $[4+2]$ cycloaddition of tetrachlorothiophene dioxide (TCTD) and *N*-ethylmaleimide (Figure 6) with multiple turnovers (45). The initially formed adduct **3** spontaneously eliminates sulfur dioxide to give *N*-ethyl tetrachlorophthalimide as the final product after oxidation in situ. The *endo* hexachloronorbornene derivative **4**, an excellent mimic of the intermediate and its flanking transition states, served as the hapten ($K_d = 2$ nM). Because the planar product is structurally so different from **4**, it binds 10^5 -fold less tightly to the induced antibody, effectively minimizing product inhibition.

In this case, catalytic efficiency can be estimated as an effective molarity (EM) (50). EM is the ratio of the pseudo-first-order rate constant for the antibody reaction (k_{cat}) to the second-order rate constant for the uncatalyzed process (k_{uncat}). This ratio gives the nominal concentration of one reactant needed to convert the spontaneous

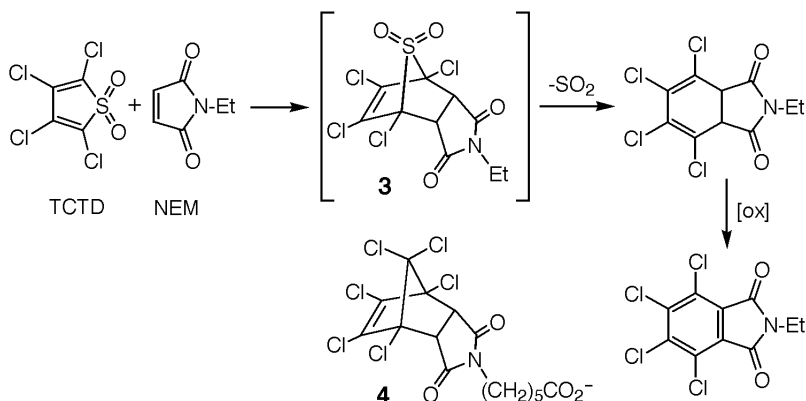


Figure 6 Diels-Alder condensation of tetrachlorothiophene dioxide (TCTD) and *N*-ethyl maleimide (NEM) yields a high-energy intermediate (**3**) that eliminates sulfur dioxide. The initially formed product is subsequently oxidized in situ. The transition states for cycloaddition and chelotropic elimination of SO_2 closely resemble the hexachloronorbornene derivative **4** used as a hapten to elicit antibody 1E9 (45).

bimolecular reaction into a pseudo-first-order process with a rate equivalent to that achieved in the antibody ternary complex. It is usually interpreted as the entropic advantage of a unimolecular over a bimolecular process, with an upper limit of about 10^8 M for 1 M standard states (51). For 1E9, the EM is $\sim 10^3$ M (52). Although much lower than the theoretical limit, this value is significantly higher than EMs reported for other antibody Diels-Alderases, which rarely exceed 10 M (46–49), making 1E9 the most efficient such catalyst described to date.

Recent structural work has shown that the 1E9 active site is exactly what one might expect of an antibody that functions as an entropy trap (52). Extensive van der Waals contacts, π -stacking interactions, and a strategically placed hydrogen bond to one of the succinimide carbonyl groups create a pocket that is highly complementary to the hapten (Figure 7a). When complexed, the ligand (excluding the hexanoate linker) is 86% buried. Its fit to the protein is so snug that no interfacial cavities are detectable, even when a probe with a 1.2-Å radius is used. Thus, the 1E9 binding pocket appears ideally suited to the task of preorganizing its diene and dienophile substrates in a reactive complex that closely approximates the transition-state geometry. Nevertheless, a simple entropy trap mechanism does not appear to be operative. The temperature dependence of k_{cat} and k_{uncat} shows that catalysis by 1E9 is achieved entirely by reducing the enthalpy of activation; the solution and the antibody processes are equally unfavorable entropically, with ΔS^\ddagger values of $-22 \text{ cal K}^{-1} \text{ mol}^{-1}$ (52). Nor is the rate acceleration due to a simple medium effect associated with the apolar binding cavity, since the uncatalyzed reaction is 10 times slower in acetonitrile than in water.

Catalysis by 1E9 can be explained by enthalpic stabilization of the transition state through an unusually close fit to the apolar binding surface of the antibody active site and a strong hydrogen bond between the side chain of Asn^{H35} and the maleimide carbonyl. Quantum mechanical calculations indicate that the numerous, energetically favorable van der Waals interactions provide the driving force for binding (52). Although these interactions distinguish poorly between ground and transition state, they hold the substrates against a relatively unfavorable electrostatic field that becomes substantially more favorable as the transition state is approached, as a result of the increased strength of the hydrogen bond to the dienophile carbonyl.

Comparison of 1E9 with another Diels-Alderase, 39-A11 (47), dramatically illustrates the importance of close packing for high efficiency. Antibody 39-A11 was generated with the substituted bicyclo[2.2.2]octene derivative **5**, which contains an ethano bridge locking the cyclohexene ring into the requisite boat conformation (Figure 8). It catalyzes the Diels-Alder reaction between an electron-rich acyclic diene and an *N*-aryl maleimide to give a cyclohexene derivative, albeit with a relatively low effective molarity of 0.35 M.

Considering the low dissociation constant reported for the antibody-hapten complex ($K_d = 10 \text{ nM}$) (47), the fit of the bicyclo[2.2.2]octene to 39-A11 is surprisingly loose (Figure 7b) (53). Only 66% of the hapten surface area is buried in the complex. Poor complementarity is indicated by the large cavity volume of 117 \AA^3

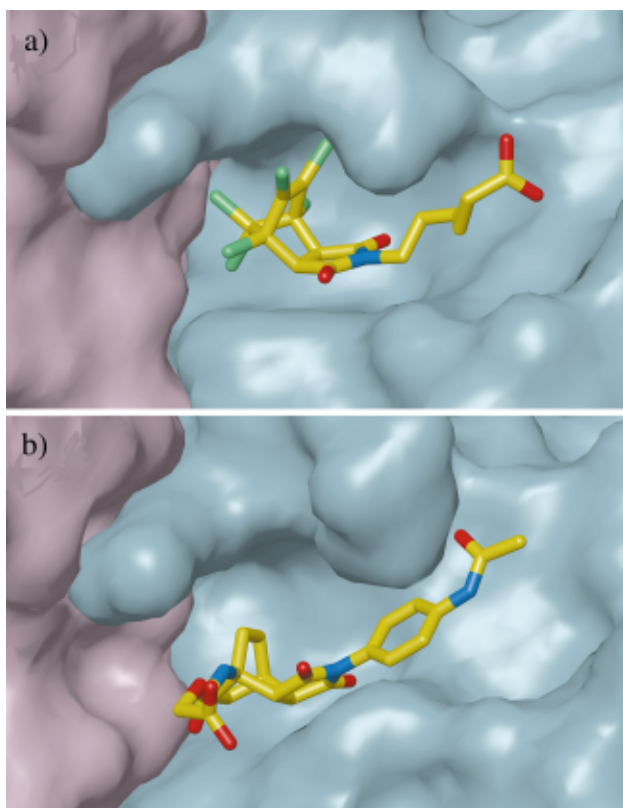


Figure 7 (a) The active site of Diels-Alderase 1E9 provides a snug, complementary binding surface for its hexachloronorbornene hapten (52). With the exception of a hydrogen bond between the deeply buried carbonyl group of the ligand and the side chain of Asn^{H35} (not shown), most of the contacts are hydrophobic in nature. (b) Antibody 39-A11 (see Figure 8) binds its hapten much more loosely. Note that the dienophile-like *N*-aryl succinimide is significantly better packed than the bicyclo[2.2.2]octene moiety, which serves as a diene surrogate.

detected between ligand and antibody. The portion of the hapten corresponding to the reacting [4 + 2] system is particularly poorly packed, whereas peripheral substituents of **5**, especially the aryl side chain, appear to be important recognition elements. Moreover, the hapten's ethano bridge, which has no counterpart in the substrates or the transition state, carves out additional unwanted space within the pocket. Consequently, the bound substrates—particularly the diene, which must bind in the least complementary region of the pocket—are likely to retain considerable degrees of freedom. Low catalytic efficiency is therefore unsurprising. Consistent with this idea, introducing large aromatic groups at positions L91 and

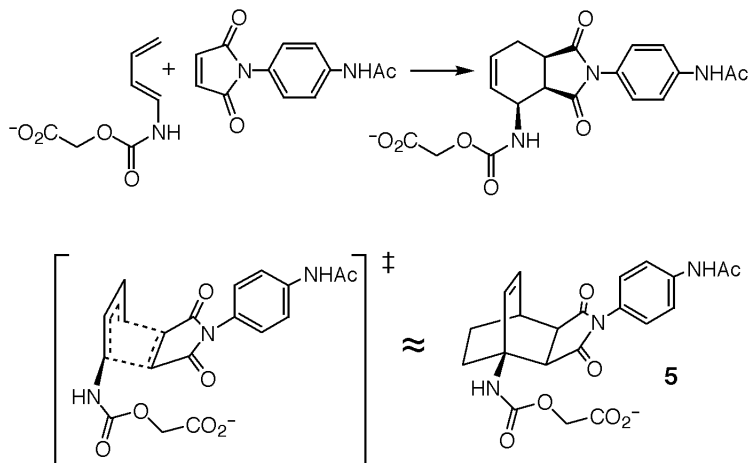


Figure 8 Antibody 39-A11 catalyzes a Diels-Alder reaction between an electron-rich acyclic diene and an *N*-aryl maleimide. It was elicited with the bicyclo[2.2.2]octene haptens **5**. The ethano bridge in **5** locks the cyclohexane ring into a boat conformation but has no counterpart in the substrate itself.

L96 to improve packing interactions with the kinetically favored *endo* transition state results in 5- to 10-fold higher k_{cat} values (54).

Relatively nonpolar as it is, the environment of the 39-A11 active site may further erode catalytic efficiency. Like 1E9, 39-A11 provides a hydrogen bond (also from Asn^{H35}) to the dienophile carbonyl, but its reaction involves a strong donor diene and acceptor dienophile rather than two electron-deficient addends. The corresponding transition state should therefore be more polar and hence more sensitive to transfer from water than that of the 1E9-catalyzed reaction. Unfortunately, mutagenesis experiments to augment activity by providing additional hydrogen bonds to the dienophile have not been successful (54).

Structurally distinct haptens notwithstanding, 1E9 and 39-A11 are unexpectedly closely related in primary sequence and tertiary structure (52, 53, 55). Both belong to a family of polyspecific antibodies that exhibit extensive cross-reactivity for hydrophobic ligands containing one or two polar groups. For example, 39-A11 and its germ line precursor accommodate a range of structurally diverse compounds (53), while 1E9 and the related progesterone-binding antibody DB3 (56, 57) bind each other's ligands with affinities only 25- to 50-fold lower than their own (55). The side chain of Asn^{H35} and conserved hydrophobic interactions seem to be particularly important for achieving recognition. However, docking experiments (52) with 1E9 and DB3 suggest that noncognate molecules bind randomly in the apolar cavity, whereas specific ligands adopt a single, well-defined binding mode similar to that seen in crystal structures of the corresponding antibody-hapten complexes. Specificity in these systems appears to be conferred by a small

number of mutations to the shared scaffold. In the case of 39-A11, for instance, substituting Val for Ser at position L91 in the germ line sequence accounts for almost all the 40-fold increase in hapten affinity achieved during affinity maturation (53). Similarly, a somatic mutation in the complementarity determining region (CDR) L3 loop (Ser^{L89} → Phe) and a rare mutation in the antibody framework region (Trp^{H47} → Leu) substantially alter the shape of the 1E9 combining pocket compared to that of 39-A11 or DB3 (52). These changes are primarily responsible for its virtually perfect shape complementarity to the transition-state analog. This complementarity appears crucial for reactivity, since DB3 does not detectably accelerate the 1E9 reaction despite its affinity for hapten **4**.

Given the enormous combinatorial diversity of the immune system [more than 10⁸ antibodies are nominally available in the primary response (58)], it is surprising that similar antibodies were generated in separate immunization experiments with **4**, **5**, and progesterone. Nor is this finding unique, as shown below. To what extent does utilization of a few restricted sets of germ line genes limit the catalytic potential of the immune system? Do these frequently selected scaffolds represent local minima from which it will be difficult to evolve more active catalysts? Poor shape complementarity between 39-A11 and the bicyclo[2.2.2]octene is a case in point. However, site-directed mutagenesis experiments demonstrate that the mature antibody is not an evolutionary dead end. The same Val^{L91}Tyr change that improves catalysis by 10-fold also increases hapten affinity 2.5 times (54), and it should be possible to find additional mutations that further tighten the structure. Because only 10 antibodies were screened for activity, we cannot know whether analogous mutations were present in the antibody population induced in response to hapten **5**. It is conceivable that they never emerged: A 10 nM dissociation constant for the 39-A11–hapten complex is more than adequate for immune system purposes, so there may be little or no selection pressure to increase affinity beyond that point.

As shown by 1E9, the combining pocket can be molded remarkably well under favorable circumstances to achieve nearly perfect shape complementarity with a ligand. Superior fit is not necessarily manifest in tighter binding, since 1E9 and 39-A11 have similar hapten affinities ($K_d = 2$ nM versus 10 nM). Compound **4** is more highly optimized than **5** with respect to transition-state mimicry, however, and important binding interactions in 1E9 are concentrated where they are needed for catalysis, rather than loosely dispersed as in 39-A11. A high degree of complementarity at the site of reaction thus appears to pay off in this case in terms of a more efficient catalytic outcome.

Even in the case of 1E9, though, much higher efficiency should be attainable. An analogous enzyme is unavailable for direct comparison [for evidence regarding possible Diels–Alderase in nature, see (59)], but the chemical proficiency of 1E9, defined as $(k_{\text{cat}}/K_{\text{diene}}K_{\text{dienophile}})/k_{\text{uncat}} = 1.4 \times 10^7$, is far from what is expected of a fully evolved catalyst. Given an already excellent fit between protein and ligand, it is unlikely that mutation of residues lining the binding cavity will substantially improve complementarity. To optimize electrostatic interactions with the transition state and reduce any remaining degrees of freedom available to the

bound substrates, residues distant from the active site will have to be modified. Because such mutations will be difficult to identify by inspection of the protein structure, combinatorial mutagenesis and an efficient screening assay (60) or selection protocol will be needed if 1E9 variants with enhanced properties are to be developed.

Strain

Substrate destabilization through strain has been proposed as another mechanism for achieving rate accelerations with enzymes (20, 61). Binding energy can be used to strain molecules in various ways. Destabilization can involve geometric distortion of the substrate, electrostatic repulsion between groups of like charge, or desolvation effects. If substrate destabilization is relieved at the transition state, significant reductions can result in the free energy of activation for reaction. Rate accelerations obtained in this way are potentially quite large, limited only by the amount of binding energy available to force the substrate into the destabilizing environment. As with entropic effects, it was predicted that strain mechanisms might be readily exploited for antibody catalysis.

Ferrochelatase Mimics Ferrochelatase is an example of an enzyme that is believed to exploit geometric distortion for catalysis. As the terminal enzyme in heme biosynthesis, it promotes complexation of Fe^{2+} by protoporphyrin IX (62, 63). Early work suggested that ferrochelatase functions by distorting the substrate porphyrin from its preferred planar conformation into a bent structure (62). This distortion exposes the nitrogen of one of the pyrroles to solvent, thereby facilitating metal ion complexation. In fact, nonplanar *N*-methylated porphyrins are known to chelate metal ions three to five orders of magnitude faster than their non-alkylated counterparts (62). They are also potent inhibitors of ferrochelatase (64). When used as haptens, they have yielded antibodies (65) that catalyze insertion of divalent metal ions into mesoporphyrins with k_{cat} values approaching those of the enzyme (Figure 9).

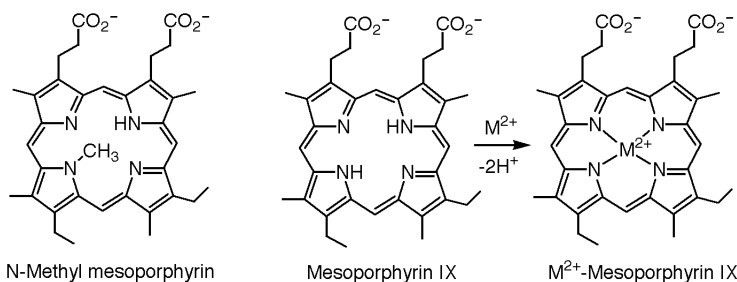


Figure 9 *N*-methyl mesoporphyrin and the mesoporphyrin metallation reaction catalyzed by antibody 7G12 (65).

Ferrochelatase antibody 7G12 has been characterized in some detail. It promotes incorporation of Zn^{2+} and Cu^{2+} into mesoporphyrin IX with k_{cat} values of 0.022 s^{-1} and 0.0069 s^{-1} , respectively (65). By way of comparison, the k_{cat} value for recombinant *Bacillus subtilis* ferrochelatase is $\sim 0.4 \text{ s}^{-1}$ for metallation with Fe^{2+} , Zn^{2+} , and Cu^{2+} (66). K_{m} values for the porphyrin are also comparable ($50 \mu\text{M}$ for the antibody and $8 \mu\text{M}$ for the enzyme). However, whereas substrate metal ions bind tightly to the enzyme ($20\text{--}170 \mu\text{M}$), no evidence for saturation of the antibody has been observed for concentrations up to 2.5 mM , suggesting that binding of metal ions to the antibody does not contribute to catalysis. Severe inhibition of the antibody-catalyzed reaction by the metalloporphyrin product is a further point of contrast.

Mechanistic and structural studies have clarified how the antibody chelatease functions. The crystal structure of 7G12 complexed with its hapten has been solved (67). The *N*-methylated porphyrin binds at the junction of the heavy and light chains (Figure 10). One face of the ligand makes extensive contacts with the variable region of the heavy chain (V_{H}), while the other is relatively exposed to solvent. Packing interactions from light chain Tyr residues may reinforce the distortion

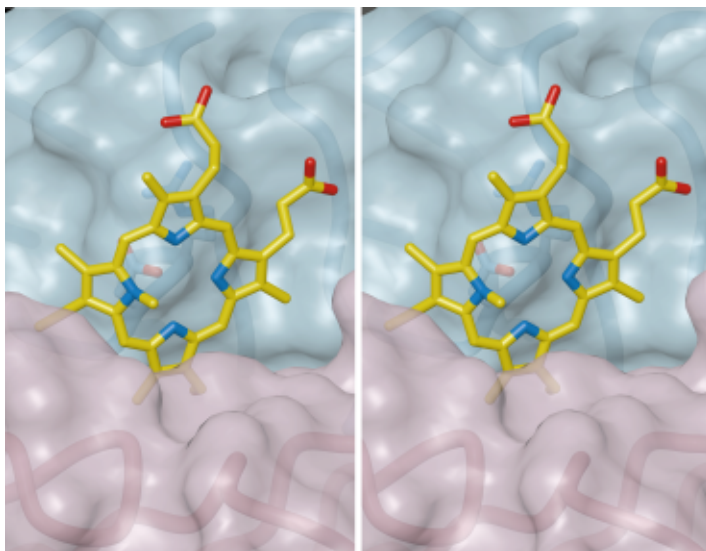


Figure 10 Stereoview of the 7G12 binding site (67), showing how bound porphyrin packs against the heavy chain (blue) and exposes one face to solvent. The side chains of heavy chain residues Asp^{H96} and Arg^{H96} are visible under the surface behind the porphyrin. Interactions with the light chain (pink) are largely restricted to contacts with the methyl and ethyl substituents of the A and B pyrrole rings of the porphyrin. Although a mixture of *N*-alkylated porphyrins was used, only the derivative with the A ring methylated appears to bind to the antibody.

from planarity of pyrrole ring A, which bears the *N*-methyl group. Replacement of these residues with Ala caused large increases in K_m and 10- to 40-fold decreases in k_{cat}/K_m (67), suggesting they may play a similar role with the nonmethylated substrate. Analogous to the enhanced reaction rates achieved by porphyrin alkylation, a catalytic mechanism involving binding and distortion of the porphyrin by the protein, followed by direct chelation of metal ions from solution, seems plausible. Although its precise role is still unclear, amino acid Asp^{H96} is evidently required for this process (67). Its carboxylate side chain is directed from the V_H domain toward the center of the porphyrin ring with one oxygen roughly equidistant to the four pyrrole nitrogens of the porphyrin (Figure 10). The other oxygen is fixed in place through a hydrogen bond to Arg^{H95}. It is conceivable that the carboxylate acts as a base that shuttles protons from the porphyrin during metal ion exchange. This residue is also probably responsible, at least in part, for product inhibition, since axial coordination to the metal ion will anchor the metalloporphyrin to the antibody.

Direct experimental evidence for porphyrin distortion by 7G12 has been obtained with resonance Raman spectroscopy (68). Spectral data show that the antibody induces an alternating up-and-down tilting of the pyrrole rings very similar to the distortion produced by porphyrin alkylation. In contrast, yeast ferrochelatase apparently causes all four pyrrole rings to tilt in the same direction in a domed fashion. The enzymatic reaction is regulated allosterically by a metal-dependent protein conformational change. Since the antibody has no metal binding site, the distortion it induces must be brought about entirely by binding interactions between porphyrin and protein. An atomic-level explanation of this effect will require elucidation of the antibody-substrate complex structure.

The broad lesson to be derived from these experiments is that substrate destabilization can be a very successful approach to antibody catalysis. Although 7G12 and ferrochelatase perturb porphyrin structure in different ways, both kinds of distortion appear to be effective for metal ion chelation, yielding k_{cat} values within a factor of 10 of each other. That said, destabilization mechanisms are expected to have little or no effect on k_{cat}/K_m (69), the steady-state parameter generally optimized through evolution. By this criterion, 7G12 is substantially more primitive than its natural counterpart. Because chelataes catalyze a bimolecular reaction, flux through the catalyst is limited by the least favorably processed substrate. For both enzyme and antibody, this is the metal ion (M^{2+}). Hence, rate enhancements are given by $[(k_{cat}/K_{M^{2+}})/k_{uncat}]$ where $K_{M^{2+}}$ is the dissociation constant of the metal ion from the protein. Since $K_{M^{2+}}$ values for 7G12 are at least 10^3 times larger than for natural ferrochelatases (assuming the metal ion binds at all), the antibody suffers an equivalent rate disadvantage under practical operating conditions, despite its favorable k_{cat} . Similar considerations apply to the chemical proficiencies of the two catalysts $[(k_{cat}/K_{M^{2+}}K_{porphyrin})/k_{uncat}]$. The affinity of the antibody for the transition state is at least four orders of magnitude lower than that of the enzyme.

To improve 7G12, a suitable binding site for metal ions should be constructed, perhaps by extending light chain CDR loops that are near the exposed face of

the bound porphyrin. The challenge will be to bring the metal ion into close proximity with the porphyrin without further increasing the affinity of the active site for product. As for the chorismate mutase antibody discussed above, an *in vivo* selection strategy is feasible. Ferrochelatase-deficient yeast auxotrophs have been reported (70). Complementing this metabolic deficiency with the antibody catalyst would provide a means of identifying more efficient variants.

Other Systems Large rate accelerations are also expected when charged reactants are enthalpically destabilized relative to a charge-delocalized transition state by desolvation (20). Such a mechanism may contribute to the efficacy of enzymes that promote biologically relevant decarboxylations (71–74). Antibody catalysis of model reactions, such as the solvent-sensitive decarboxylation of 3-carboxy-benzisoxazoles to salicylonitriles (75, 76) and the difficult decarboxylation of orotate to uracil (77), has been used to probe the role of medium effects in a tailored binding pocket. Significant rate enhancements have been achieved and structural work characterizing the properties of successful active sites will be instructive. Given the well-established and often dramatic sensitivity to solvent change of many reaction types, medium effects are likely to be pervasive in antibody and enzymatic catalysis. Reactions that display large changes in charge localization, including decarboxylations, hydrolyses, nucleophilic substitutions, and aldol condensations, should be especially amenable to such effects.

Electrostatic Catalysis

Acyl Transfer Reactions Enzymes frequently use hydrogen bonding and charged groups to stabilize polar transition states electrostatically (69). When haptens containing positive and negative charges are used, electrostatic interactions can also be exploited for antibody catalysis. For example, anionic phosphonates and phosphoramidates, originally designed as potent inhibitors of hydrolytic enzymes (12, 78), have been useful in the production of antibodies that hydrolyze esters, carbonates, and (more rarely) amides (79). Such analogs resemble the transition state for hydrolysis in a number of ways, including tetrahedral geometry, negative charge, and increased bond lengths. How these features are reflected in the induced binding pockets has been deduced through structural studies of six independently derived esterases (80–90).

Antibody 48G7 is typical of this class of catalyst (91). It was generated against *p*-nitrophenyl phosphonate **6** and accelerates the hydrolysis of the corresponding activated ester **7a** and carbonate **7b** by factors of 1.6×10^4 and 4×10^4 , respectively (Figure 11). Both the antibody and its germ line precursor, with and without bound hapten, have been characterized to provide insight into the origins and evolution of its catalytic effects (85–87).

The mature antibody has a deep, well-defined combining site rich in aromatic residues (Figure 12a). It binds the hapten in an extended conformation with the aryl group at the bottom of a hydrophobic cleft formed between CDRs L1 and H3.

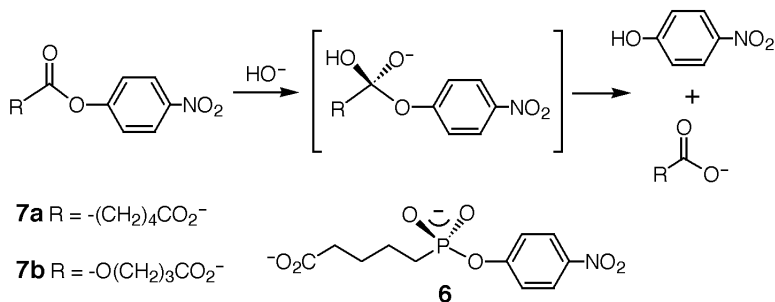


Figure 11 Hydrolysis of activated aryl esters **7a** and carbonates **7b** proceeds via an anionic and tetrahedral intermediate (*in brackets*). Hydrolytic antibody 48G7 was elicited with an aryl phosphonate derivative **6** that mimics this high-energy species and its flanking transition states (91).

The negatively charged phosphonate moiety lies near the pocket entrance, where it forms multiple interactions with charged and neutral antibody residues. The pro-R phosphonyl oxygen forms a hydrogen bond with the Tyr^{H33} phenolic hydroxyl group and a salt bridge with the Arg^{L96} guanidinium group, while the pro-S oxygen forms hydrogen bonds to the His^{H35} ϵ -imino group and the Tyr^{H96} backbone amide. Comparison of the mature antibody with and without the transition-state analog shows no major conformational changes (86), suggesting a simple lock-and-key mechanism for hapten binding (however, see 92).

Antibody 48G7 has a 30,000-fold higher affinity for the phosphonate hapten and 20-fold greater catalytic efficiency than its germ line precursor. Nine somatic mutations, all lying outside the combining site, are responsible for these effects (85, 87, 93). Although not in direct contact with bound ligand, the mutated residues appear to preorganize the pocket for binding and catalysis. Improved packing and secondary hydrogen-bonding interactions help limit the side chain and backbone flexibility inherent in the germ line protein. In fact, germ line 48G7 (Figure 12*b*) is conformationally much more flexible than the mature antibody and undergoes significant reorganization upon hapten binding (87). The hapten itself binds quite differently in the two complexes (Figure 12*a, b*). The phosphonate moiety occupies essentially the same location in both, but it cannot form a hydrogen bond with Tyr^{H33} in the germ line complex, owing to an altered conformation of the CDR H1 loop. Further, the *p*-nitrophenyl group is rotated away from the position it adopts in the mature antibody to occupy a hydrophobic cleft constructed from framework residues. This second apolar pocket is present, but empty, in mature 48G7. The alternative binding mode is made possible by removal of an otherwise repulsive interaction with the nitro group of the hapten in the mature antibody by the somatic mutation Ser^{L34}Gly.

Concordant with hapten design, the crystallographic data suggest that 48G7 is a relatively simple catalyst that promotes ester hydrolysis by direct attack of

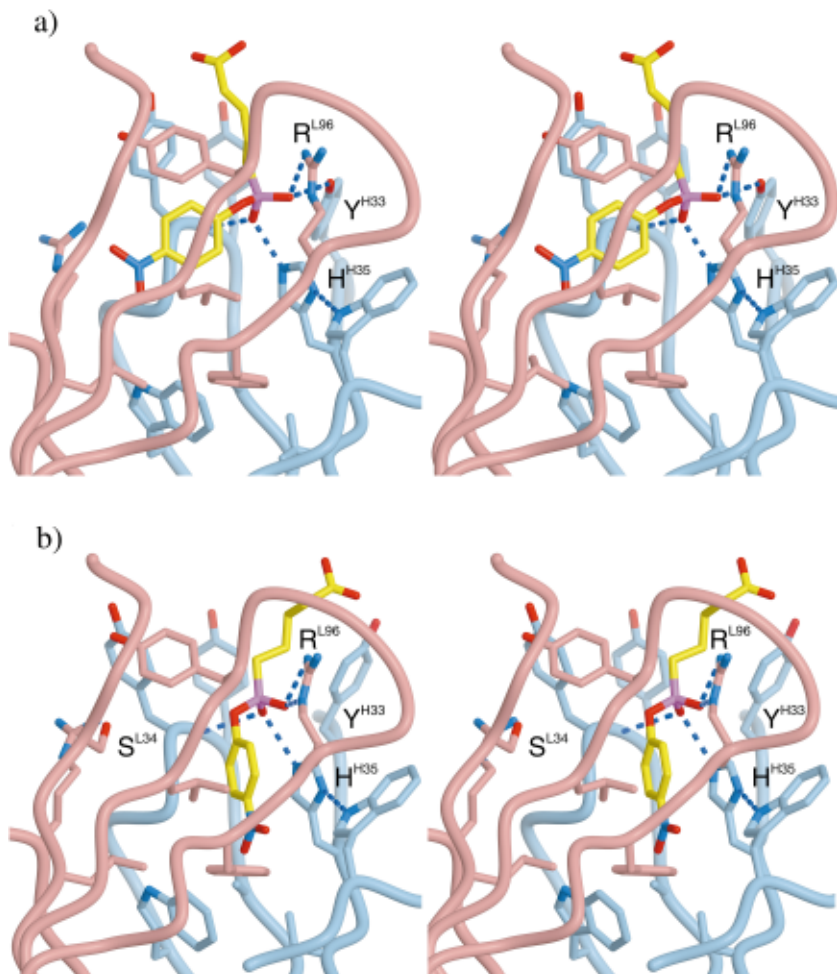


Figure 12 Stereoview of the active site of mature 48G7 (*a*) and its germ line precursor (*b*) showing the different orientation of the hapten in the two complexes (85–87). The phosphonate moiety of **6** binds in roughly the same location in both, although the network of hydrogen bonding interactions that constitute the oxyanion hole is slightly different. The deeply bound aryl group binds in one of two available hydrophobic clefts at the bottom of the pocket depending on whether the residue at position L34 is Ser (germ line) or Gly (mature).

hydroxide on the scissile carbonyl. Although the two hapten binding modes seen in the germ line and mature 48G7 complexes create some ambiguity about the preferred orientation of the substrate, the side chains of Tyr^{H33}, His^{H35}, and Arg^{L96} and the backbone amide of Tyr^{H96} apparently stabilize the tetrahedral and anionic transition states electrostatically through hydrogen bonding and ionic interactions

(Figure 12). An analogy between this anion binding site and the well-characterized oxyanion hole of serine proteases is apparent. Individually, however, the antibody residues are not very effective oxyanion stabilizers. Mutations at positions H33, H35, and L96 cause only 3- to 30-fold reductions in k_{cat} (85). Loss of the hydrogen bond between Tyr^{H33} and the transition state probably contributes to the 20-fold lower efficiency of the germ line, as well. In contrast, replacement of a single asparagine in the oxyanion hole of the protease subtilisin results in 10²- to 10³-fold losses in specific activity (94, 95). High solvent accessibility or conformational mobility of the antibody residues may account for their limited efficacy.

The 48G7 active site structure and hapten-recognition properties are strikingly similar to those of other, independently generated antiphosphonate antibodies (96). These include three catalysts [CNJ206 (80, 81), 17E8 (89), and 29G11 (90)] for the cleavage of (*p*-nitro-)phenyl esters and three [D2.3, D2.4, and D2.5 (83, 84)] for the energetically more demanding hydrolysis of *p*-nitrobenzyl esters. Although many of these esterolytic antibodies derive from different germ line sequences, they appear to have in common a deep hydrophobic pocket in the framework region into which the aryl/benzyl ring of the leaving group binds (Figure 13). All exploit multiple hydrogen bonds and salt bridges near the mouth of the cavity for recognition of the phosphonate moiety. Consequently, it is likely that all employ the same basic hydrolytic mechanism as 43G7 (96). Given this, their comparative

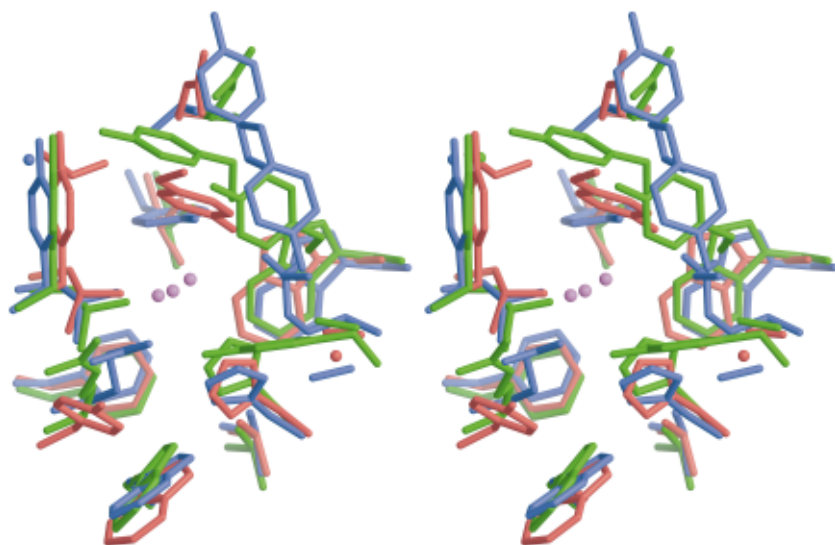


Figure 13 Overlay of three hydrolytic antibodies, 48G7 (*green*), 17E8 (*blue*), and CNJ206 (*red*), shows remarkable structural convergence in these independently generated active sites (96). Only hapten-contacting side chains are illustrated; the *purple balls* indicate the position of the phosphorus of the respective bound hapten.

efficiency, which ranges over two orders of magnitude, must reflect differing abilities to stabilize the hydrolytic transition state relative to the bound ground state. Examination of the hapten complexes suggests that the rate enhancement ($k_{\text{cat}}/k_{\text{uncat}} = 10^3$ to 10^5) roughly parallels the number of hydrogen bonds to the phosphonate. Flexibility in the active site (as seen in the 48G7 germ line antibody) also correlates with low efficiency (80, 81, 87). In some cases, the antibodies may exploit binding energy to distort the substrate ester from its thermodynamically favorable Z conformation, making it easier to reach the tetrahedral transition state during catalysis (82, 85). For example, this factor may come into play in 48G7, depending on whether the substrate binds like the hapten in the mature or the germ line complex (Figure 12).

The remarkable degree of structural convergence observed in antibodies selected for tight binding to aryl phosphonate transition-state analog finds parallels in a number of other systems. For example, the immune responses to phosphorylcholine (97), *p*-azophenylarsonates (98), and 2-phenyloxazolones (99) are dominated by specific combinations of heavy and light chain variable regions. Interestingly, when a phenyloxazolone-binding antibody was found with a unique V_{H} domain, its structure showed conservation of important antigen binding residues (100). These results point to the immune system's use of a relatively limited number of mechanisms to recognize any given type of antigen. Apparently, strong selective pressure reduces the broad diversity initially present in the primary repertoire to a small set of "best" solutions that can be further optimized by somatic mutation. As discussed above for the Diels-Alderases, structural convergence is even evident in antibodies raised against unrelated haptens. Rather than possessing an infinite variety of differently configured active sites, the immune system appears to play with a limited deck.

Variations within the general theme do arise. Another esterase that has been structurally characterized, antibody 6D6, catalyzes the hydrolysis of a chloramphenicol monoester with relatively low efficiency ($k_{\text{cat}}/k_{\text{uncat}} = 900$) (101). It shows specific differences from the other antibodies (82). In particular, the hapten is bound more shallowly, although the stacked aromatic rings of the leaving group and the acyl side chain are the most deeply buried portions of the molecule. The tetrahedral phosphonate is highly solvent exposed, forming only one hydrogen bond to the antibody, presumably explaining the relatively low efficiency of 6D6.

At this point, it is not clear how much activity can be obtained from antiphosphonate antibodies. Over 50 esterolytic antibodies have been shown to have properties roughly comparable to those discussed here: simple hydrolytic mechanisms, rate accelerations up to 10^5 over background, and chemical proficiencies of 10^7 to 10^8 M^{-1} (15, 16). While notable, particularly considering concomitant high and predictable selectivity (3), such effects are still orders of magnitude lower than those achieved by analogous enzymes. The immunological approach appears to have hit a ceiling in catalytic efficiency. It seems likely that these activities reflect what can be achieved with an oxyanion hole mechanism alone. Recent attempts to augment activity by rational mutagenesis or affinity selection with phage-displayed

antibody fragments have met with only limited success (102–105). Negative results should not be overinterpreted, but they do raise concerns that the aryl phosphonate binding pocket common to these catalysts is not an intermediate that can be further refined but an evolutionary dead end. Alternative strategies for antigen presentation and methods for in vitro selection may provide access to different subsets of the immune repertoire more amenable to optimization. For example, antibodies that bind tetrahedral anions not at the entrance to the combining site but deep within their active site, as seen for enzymes that promote hydrolyses, would be of interest.

Of course, highly evolved hydrolytic enzymes are more than simple oxyanion holes. They exploit arrays of catalytic groups (and, often, metal cofactors) to catalyze energetically demanding reactions such as amide hydrolysis. Induction of several precisely aligned functional groups in a single immunization step is extremely improbable, however. Such arrays are unlikely to be present in the primary repertoire of the immune system, and depending on the basic immunoglobulin scaffold, they may not be accessible through somatic hypermutation. Occasionally, though, serendipitous mutations that open new opportunities for catalysis can and do occur.

Although phosphonate transition-state analogs specify a simple hydrolytic mechanism, some antiphosphonate antibodies have been identified that exploit more complex mechanisms. For example, the lipase-like antibody 21H3, generated against a typical benzyl phosphonate ester (106), unexpectedly accelerates ester hydrolysis by a two-step mechanism involving transient acylation of an amino acid within the binding pocket (107). Its efficiency at hydrolyzing esters is no greater than that of the esterolytic antibodies discussed above, but use of covalent catalysis makes possible stereoselective transesterification reactions that cannot be carried out in water without the antibody (107, 108). Similarly, considerable biochemical evidence has been adduced for a two-step sequence involving an acyl-antibody intermediate in hydrolytic reactions catalyzed by antibody 43C9 (109). The latter was generated against phosphoramidate **8** (110), rather than a phosphonate, and it is unique in its ability to promote the hydrolysis of activated amides as well as esters (Figure 14). A 2.5×10^5 -fold rate enhancement (chemical proficiency =

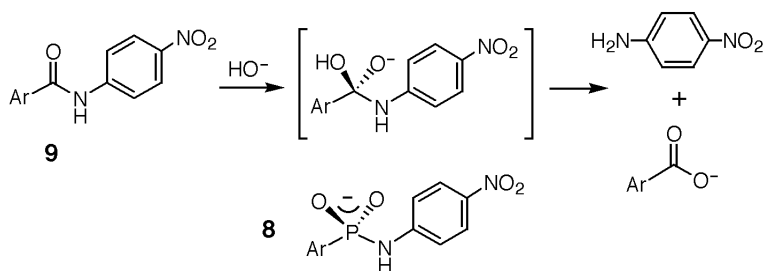


Figure 14 Phosphoramidate **8**, which is a transition-state analog for amide hydrolysis, yielded antibody 43C9 (110). This antibody cleaves structurally related *p*-nitroanilides **9** and esters (not shown).

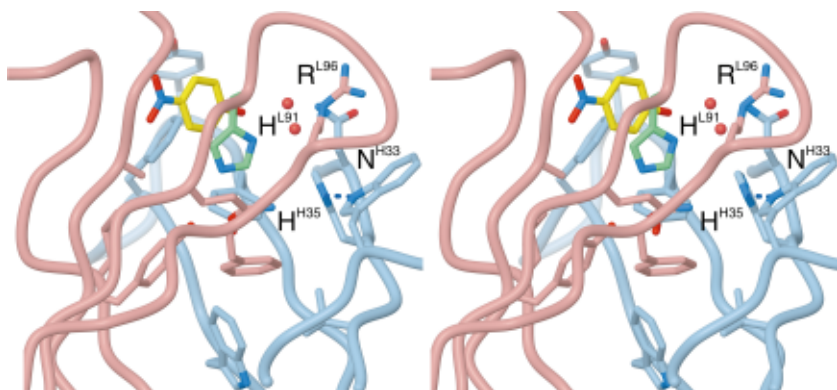


Figure 15 Stereoview of the active site of amidase 43C9 with bound *p*-nitrophenol (88). The imidazole side chain of His^{L91} (green) points into the pocket toward the region normally occupied by the phosphonate in other hydrolytic antibodies. Asn^{H33}, His^{H35}, and Arg^{L96} are potential oxyanion stabilizers. Two water molecules in the active site are shown as red spheres.

$5 \times 10^8 \text{ M}^{-1}$) achieved in the cleavage of *p*-nitroanilide **9** makes 43C9 one of the most efficient hydrolytic antibodies known.

The crystal structures of free 43C9 and its complex with *p*-nitrophenol were recently solved (88). Although detailed understanding of interactions specific to ligand recognition and catalysis await characterization of the haptene complex, likely participants in the reaction are identifiable upon inspection of the binding pocket (Figure 15). As with other hydrolytic antibodies, several residues are available for stabilizing the negative charge that develops in the transition state, many of which are shared with 48G7. These include His^{H35} and Arg^{L96}, whose importance for catalysis is supported by the results of site-directed mutagenesis experiments (103). Residue Asn^{H33}, like Tyr^{H33} of 48G7, may also play a role in transition-state stabilization. What distinguishes 43C9 from other esterolytic antibodies, though, is the presence of a second histidine at position L91. His^{L91} is directed into the pocket toward the region where substrate must bind (Figure 15). Docking experiments have suggested a plausible orientation of the substrate in which its scissile carbonyl is in excellent position for nucleophilic attack by the imidazole side chain of His^{L91} (88). Detailed mechanistic inferences should be considered tentative in light of likely perturbations to the binding pocket caused by packing interactions between the active sites of adjacent molecules in the crystal (88). Nevertheless, mutagenesis of His^{L91} to Gln decreases catalytic efficiency >50-fold with little effect on ligand binding, supporting its role as the nucleophile that is transiently acylated during catalysis (103). Consistent with this possibility, the acyl intermediate detected by electrospray mass spectrometry at pH 5.9 is not observed with the His^{L91}Gln variant (111).

Covalent catalysis by imidazole is well established in nonenzymatic reactions of carboxylic acid derivatives (1). Its efficiency is a consequence of the high nucleophilicity of imidazole and the relative instability of the acyl-imidazole intermediate. The presence of His^{L91} can thus explain why 43C9, but not 48G7 or other esterolytic antibodies, cleaves an amide. Context is clearly relevant, since lipase 21H3 lacks amidase activity though it also exploits nucleophilic catalysis (106, 107). The fact that the mechanism of 43C9 is unspecified by the design of its hapten also underscores the importance of serendipity in these experiments. The rarity of such occurrences is reflected in many failed experiments to generate amidases with phosphoramidate haptens.

Despite its relative mechanistic sophistication, 43C9 is still a primitive amidase when compared with a typical protease. Subtilisin, which also exploits nucleophilic catalysis, catalyzes the cleavage of succinyl-Ala-Ala-Pro-Phe-*p*-nitroanilide 10^4 times more efficiently than 43C9. Its rate acceleration is 3.9×10^9 over background and its chemical proficiency is $2.2 \times 10^{13} \text{ M}^{-1}$ (112). Moreover, subtilisin can cleave unactivated amides, whereas 43C9 is restricted to substrates with leaving groups of $\text{pK}_a < \sim 12$ (113).

The high efficiency of covalent catalysis in serine proteases like subtilisin derives from cooperative action of several functional groups in addition to the active site nucleophile. Acid-base chemistry, in particular, is used to activate the serine nucleophile, facilitate proton transfers, and stabilize the amide leaving group. Removal of any single component of the protease catalytic triad results in 10^4 - to 10^6 -fold decreases in activity (112). Unsurprisingly, 43C9 lacks an analogously complex catalytic machinery. Although it has proved difficult to install additional functional groups by mutagenesis (103), more productive changes may become obvious when the structure of the hapten complex is known. Lessons from the immunological evolution of 48G7 (53, 87) suggest that mutagenesis of residues outside the binding pocket will be required to fine-tune critical synergies between participants in catalysis.

Functional Groups

Functional groups—nucleophiles, acids, bases, and even exogenous cofactors—can clearly extend the capabilities of catalytic antibodies. They will certainly be needed if reactions with large activation barriers are to be significantly accelerated. As we have seen in the case of amidase 43C9, unplanned but useful residues can appear by chance in the immunoglobulin pocket during affinity maturation. To increase the probability of eliciting such functional groups where they are needed, several strategies have been devised.

Charge complementarity between an antibody and its ligand is the easiest principle to exploit in generating functionalized binding pockets. Cationic haptens have been used, for instance, to elicit negatively charged carboxylates that can serve as bases or nucleophiles or as general acids when protonated. Elimination

reactions, epoxide ring openings, cationic cyclizations, and hydrolyses of esters, ketals, and enol ethers have been successfully catalyzed by this approach (114). In favorable cases, very large catalytic effects have been achieved. For example, antibodies raised against a protonated benzimidazolium derivative use an active site Asp or Glu to deprotonate substituted benzisoxazoles with effective molarities of 40,000 M and rate accelerations in excess of 10^8 over the acetate-promoted background reaction (115).

Nevertheless, it is unlikely that a single hapten will ever elicit arrays of residues as sophisticated as those present in highly evolved enzymes. Heterologous immunization has been explored as a method of circumventing this limitation (116). In this procedure, two molecules, each containing different functional groups, are serially used as haptens to elicit the immune response. Ideally, a subset of the resulting antibodies will possess multiple catalytic groups induced in response to both templating molecules and have, as a result, enhanced activities. An important advantage of this strategy is that simplified haptens can be used, reducing the need for laborious synthesis. Although generality must still be established, results from initial studies indicate that antibody esterases generated by heterologous immunization are more efficient than those generated in response to the individual haptens (116, 117).

Mechanism-based enzyme inhibitors (17, 18) are potentially of even greater utility as haptens (19, 118–122). Such molecules exploit the ability of a protein to initiate a cascade of events ultimately leading to its own covalent modification. This irreversible chemical reaction thus provides a means of selecting immunoglobulins *in vivo* or *in vitro* on the basis of their activity. When the selected antibody is challenged with substrate rather than hapten, the same group(s) responsible for protein modification can be used to promote the desired chemical transformation. Covalent catalysis can thus be specified through hapten design. The potential of reactive immunization is perhaps best illustrated by the production of aldolase antibodies (120). These catalysts not only use a complex chemical mechanism but are among the most efficient catalytic antibodies described to date.

Aldolases Aldol condensations are broadly useful in organic synthesis as reactions for forming carbon-carbon bonds. They pose special difficulties for biocatalysts, however, because they proceed via a series of consecutive transition states, each requiring acid-base catalysis. Class I aldolases solve these problems by using a reactive lysine to activate the ketone donor through Schiff base formation at the active site (123–125). Deprotonation of the Schiff base yields an enamine that then adds stereoselectively to the acceptor aldehyde to form a new carbon-carbon bond. Subsequent hydrolysis of the Schiff base releases product and regenerates the active catalyst.

β -Diketones inhibit class I aldolases by forming a Schiff base with the active site lysine and then rearranging to a more stable vinylogous amide. When β -diketone **10** was used as a hapten instead of a more conventional transition-state analog

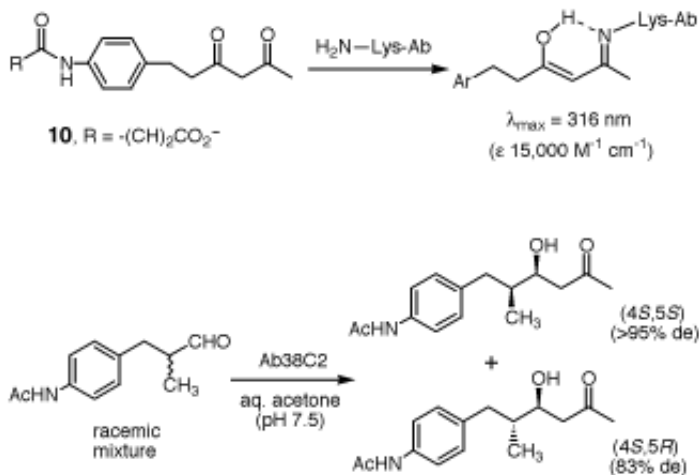


Figure 16 β -Diketone **10**, used as a hapten to raise antibodies 38C2 and 33F12, traps a reactive, active site amine to form a stable, chromophoric vinylogous amide (**120**). These antibodies promote diverse aldol condensations. In the example shown (*bottom*), the two products are formed in a ratio of about 1:1 with the indicated diastereoselectivities.

(**120**), two analogously modifiable antibodies (33F12 and 38C2) were obtained (Figure 16). The reactive group on the antibodies is a lysine with an anomalously low pK_a [5.5 for 33F12 and 6.0 for 38C2 (123)]. The vinylogous amide it forms with the hapten (λ_{max} 316 nm, ϵ 15,000 $\text{M}^{-1} \text{ cm}^{-1}$) can be irreversibly trapped by reduction with sodium cyanoborohydride. These same antibodies also mimic the activity of class I aldolases (**120**). Their reactive lysine reacts with a wide range of ketones to form enamine adducts. These condense with diverse aldehydes to form aldol products.

The structure of antibody aldolase 33F12 (**123**) shows the catalytic lysine (Lys^{H93}) buried at the bottom of a hydrophobic pocket (Figure 17). It is not hydrogen bonded with other amino acids and there are no charged residues within 7 Å. The absence of such interactions must be responsible for the unusual reactivity of this group: The hydrophobic microenvironment lowers the pK_a of the amine by disfavoring the protonated state. In contrast, class I aldolases are believed to increase the acidity of their catalytically essential lysine through proximity to several positively charged residues (**126**).

Unfortunately, the unliganded antibody provides few clues about the interactions that stabilize the transition states for formation and breakdown of the carbinol amine, deprotonation to afford the enamine, and creation of the new carbon-carbon bond. Sequestered water molecules or the hydroxyl groups of Tyr or Ser residues that constitute the pocket walls may be involved. For instance, a simple rotation

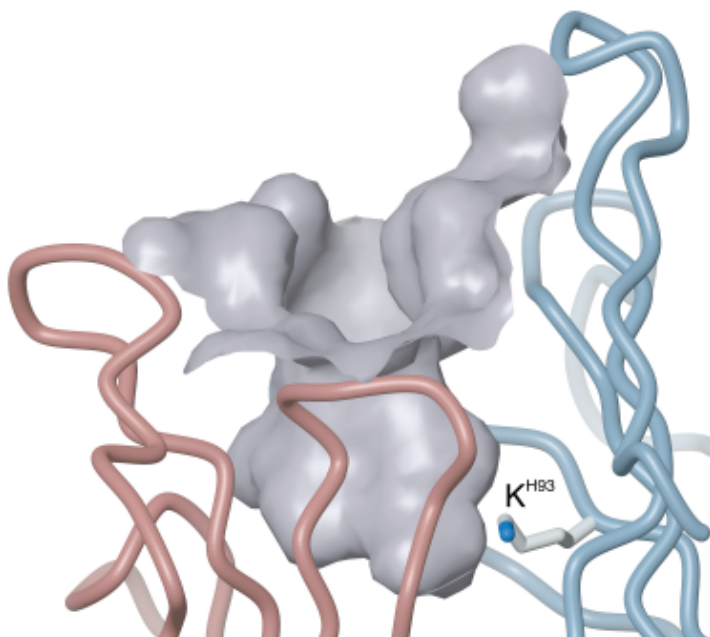


Figure 17 The binding pocket of antibody 33F12 (123) is seen through a slice in the molecular surface calculated with a sphere of 1.4 Å radius (206). Only the ϵ -amino group of Lys^{H93} contacts the molecular surface at the bottom of the antigen binding site.

of the Lys side chain from its position in the unliganded antibody would bring its amino group near Ser^{H100}, which lies on the opposite side of the pocket. Structures of enamine adducts will be important for clarifying these points.

An unanticipated feature of the aldolase antibodies is their promiscuity. Over 100 different reactions, including aldehyde-aldehyde, ketone-aldehyde, and ketone-ketone condensations, are subject to catalysis (123). Because the 33F12 pocket is relatively hydrophobic, polyhydroxylated aldehydes, such as glyceraldehyde, glucose, and ribose, which are good acceptors for natural aldolases, are not substrates for the antibodies. Aside from this restriction, a wide range of donors and acceptors is tolerated. Nonspecific van der Waals interactions likely provide the driving force for sequestering the first substrate. Once bound, it encounters the reactive lysine and forms the nucleophilic enamine. Provided there are no steric clashes, similar interactions should allow the aldehyde acceptor to bind and undergo aldol addition. The binding site is 11 Å deep and quite capacious, much larger in fact than the β -diketone site that induced it, accounting for this broad specificity. These properties have been rationalized as a consequence of the reactive immunization process itself (123): Capture of the antibody by a covalent chemical event early in

the process of affinity maturation may obviate the need for further refinement of the binding pocket by somatic mutation.

Although induced with an achiral hapten and despite their broad substrate specificity, these aldolase antibodies are surprisingly stereoselective (Figure 16). When acetone is the donor substrate, addition preferentially occurs on the *si*-face of the aldehyde acceptor; with hydroxy acetone, attack occurs on the *re*-face. In most cases, enantiomeric excesses >95% are found (127). Enantioselective Robinson annulations (128), resolution of tertiary aldols (129), and preparation of chiral intermediates for the total synthesis of brevicomins (130) and ephothilones (5) illustrate the synthetic utility of these catalysts. Kinetic resolution of the ephothilone precursor was carried out on a gram scale using 0.06 mol% of antibody 38C2 (corresponding to 0.5 g of IgG). The reaction proceeded with good yield (37%) and high enantiomeric excess (90%). More recently, antibody 38C2 has been used to activate prodrugs (6). It catalyzes the selective removal of generic drug-masking groups via sequential retroaldol and retro-Michael reactions. This advance could prove useful in the development of selective chemotherapeutic strategies.

How do these remarkable antibody aldolases measure up to natural aldolases? To address this question, it is easiest to consider representative retroaldol reactions. For such transformations, the antibodies achieve turnover numbers ranging from 0.0003 to 0.08 s⁻¹ (127). One of the best antibody substrates is 4-(4'-isobutyramidophenyl)-4-hydroxy-2-butanone. In the presence of 38C2, it undergoes retroaldolization with k_{cat} and $k_{\text{cat}}/K_{\text{m}}$ values of 0.083 min⁻¹ and $3.3 \times 10^3 \text{ M}^{-1} \text{ s}^{-1}$, respectively. The rate constant for the background reaction is $1.4 \times 10^{-9} \text{ s}^{-1}$ (aqueous buffer, pH7, and 25°C). The antibody thus accelerates this reaction by a factor of 2×10^7 -fold; its chemical proficiency is $6 \times 10^{10} \text{ M}^{-1}$. These are impressive effects for a catalytic antibody, and may be compared with activity accruing to FDP aldolase and KDPG aldolase, typical class I enzymes involved in sugar metabolism.

FDP aldolase catalyzes the interconversion of fructose-1,6-diphosphate (FDP) to give dihydroxyacetone phosphate and glyceraldehyde-3-phosphate. Its steady-state kinetic parameters in the cleavage direction are $k_{\text{cat}} = 48 \text{ s}^{-1}$ and $k_{\text{cat}}/K_{\text{m}} = 1.6 \times 10^7 \text{ M}^{-1} \text{ s}^{-1}$ (131). KDPG aldolase, which cleaves 2-keto-3-deoxy-6-phosphogluconate (KDPG) into pyruvate and glyceraldehyde-3-phosphate, is even more active, having k_{cat} and $k_{\text{cat}}/K_{\text{m}}$ values of 290 s⁻¹ and $4.0 \times 10^6 \text{ M}^{-1} \text{ s}^{-1}$, respectively (132). Although rate constants for the corresponding uncatalyzed reactions are unavailable, taking $1.4 \times 10^{-9} \text{ s}^{-1}$ as a conservative estimate (127) yields rate enhancements of $\sim 10^{10}$ to 10^{11} and chemical proficiencies of $\sim 10^{15}$ to 10^{16} M^{-1} . By either criterion, the natural enzymes are several orders of magnitude more efficient than the antibody aldolases.

Natural aldolases are more restrictive in their substrate requirements than the antibodies, though they could lose considerable activity and still be competitive. For example, removal of a single phosphate in FDP causes a 50-fold loss in rate

with FDP aldolase (131). The extensive interactions that confer such specificity are almost certainly coupled to the high efficiency of the enzyme. By further refining the antibody pocket to the precise steric and electronic demands of a particular aldol reaction, while maintaining the high reactivity of the active site lysine, enzyme levels of activity may be attainable. Narrowed scope may be the unavoidable cost of truly high efficiency, however.

PERSPECTIVES

General Lessons from Comparisons of Enzymes and Antibodies

Structural and mechanistic work reviewed here reveals many notable parallels between antibodies and their more highly evolved counterparts. Not only are the sizes and shapes of their active sites comparable, but antibodies and enzymes use the same set of molecular interactions to bind their respective ligands and stabilize transition states. Although antibodies tend to be less extensively functionalized than enzymes, the basic mechanistic strategies they employ to lower kinetic barriers are strikingly similar. As more primitive catalysts, however, they provide an alternative vantage point for examining the relationship between binding energy and catalysis. In this regard, simplicity is a virtue. Rather than working backward from a fully evolved enzyme, uncomplicated model systems can be constructed to illuminate specific mechanistic questions. As multiple mechanistic strategies are combined to augment efficiency, valuable insight into the evolution of catalytic function can be gained. Functional analysis of the antibody intermediates that arise during affinity maturation (38, 53, 85, 87) also sheds light on these issues.

Currently, antibodies appear less successful than enzymes in their ability to achieve the fine level of recognition required for optimal discrimination between transition states and ground states (12). Their modest efficiencies appear to be a direct consequence of the simple strategy used to generate them. Whereas the process of natural selection optimizes enzymes on the basis of their catalytic activity, the microevolutionary mechanisms of the immune system select antibodies for increased affinity to an imperfect transition-state analog. It is unrealistic to expect that proteins engineered to recognize such haptens will provide an ideal steric and electrostatic environment for chemical transformation. Even with a perfect transition-state analog, the chances of obtaining a fully evolved catalyst through immunization would be low. As noted above, selection pressure is generally insufficient to attain the high binding energies that characterize complexes between true enzymes and their transition states. On both micro and macro levels, mechanistic improvements arise as a function of time, so differences in time scales for the evolution of enzymes and antibodies—millions of years versus weeks or months—also come into play.

Although nature uses a wide variety of different protein scaffolds to build enzyme active sites (133), it does not seem to have adopted the immunoglobulin fold. It is therefore conceivable that antibody structure itself places intrinsic limitations on the kind of reactions amenable to catalysis and on attainable efficiencies. In general, though, structural studies show excellent shape and chemical complementarity between antibodies and their ligands. Depending on the hapten, deep pockets, clefts, grooves, and flatter, more undulating surfaces can be created (134, 135). Because certain classes of haptens tend to be recognized in the same way (52, 53, 83, 96), structural diversity must be considerably more restricted than might have been expected given 10^8 variants available in the primary immune repertoire (136, 137), but whether these consensus sites significantly restrict the catalytic capabilities of antibodies is still unclear.

Conformational flexibility is another potential concern. Protein conformational changes in enzymes provide a means of excluding water from the active site and enable the catalyst to adjust to changes in substrate as the reaction coordinate is traversed (138, 139). Antibodies are known to undergo a comparable range of ligand-induced conformational changes, including alterations in side chain rotamers, segmental movements of hypervariable loops, and changes in the relative disposition of the V_H and V_L domains (134). Without direct selection for activity, however, these dynamic effects will be difficult to exploit deliberately for catalysis. In fact, conformational flexibility in catalytic antibodies, when observed (80, 81, 87), usually results in lower rather than higher efficiency.

How Efficient Does Catalysis Need to Be?

Enzymes represent an extraordinarily high standard against which to judge new catalysts that are rationally designed from simple principles. From the perspective of the chemist, one exciting aspect of catalytic antibody technology is its ability to deliver tailored catalysts for reactions that are difficult to carry out selectively using existing methods or for which natural enzymes do not exist. Must such systems attain enzymelike efficiency to be useful?

Because antibodies are biocompatible and have long serum half-lives, many *in vivo* applications would be conceivable if sufficient activity were available. In fact, existing catalytic antibodies have already achieved significant effects in biological systems. When expressed at high levels, they have been shown to be competent (if inefficient) catalysts in metabolism, replacing essential enzymes in amino acid (42) and pyrimidine biosynthesis (77) pathways. Therapeutically relevant concentrations of the aldolase antibodies discussed earlier have been used to activate prodrugs and kill colon and prostate cell lines (6). Similarly, an esterolytic antibody has been employed as a cocaine antagonist, protecting rats from cocaine-induced seizures and sudden death (140, 141).

Many chemical reactions cannot proceed in the absence of catalysts because competing pathways have lower energies. In several instances, antibody binding

energy has been successfully used to alter the course of such reactions by selectively stabilizing the less favorable transition state. For example, antibody catalysts have been developed for normally disfavored *syn*-eliminations (142), *exo* rather than *endo* Diels-Alder cycloadditions (46, 48), and 6-*endo*-tet ring closures of epoxy alcohols (143, 144). Antibodies have also been used to control the fate of high-energy intermediates, allowing them to partition along only one of several possible pathways, as in the case of conversion of an enol ether to a cyclic ketal in water (145). Formation of a strained cyclopropane derivative in a cationic olefin cyclization is another such example (146). Binding energies up to 5.5 kcal mol⁻¹ are typically available for achieving such discrimination, and even more energy may be available in favorable cases (15). Such selectivities could be of great utility in organic synthesis.

Assuming an antibody is available for a particular transformation, its turnover and cost will ultimately determine whether it is used in practice. Presently, the steady-state parameters of typical catalysts necessitate high antibody concentrations ($\geq 10 \mu\text{M}$, or 1.6 mg/ml) and long reaction times to achieve useful conversions (12). Preparative applications of several antibodies show that gram-scale reactions are feasible, particularly if antibody selectivity is high and competing reactions are substantially slower than the desired transformation (5, 147, 148). Costs associated with high-volume antibody production are certainly an issue, but some antibodies are now produced on a large scale for diagnostic and medical applications. They are readily obtained in good yield through ascites production (149) or by fermentation in hollow fiber reactors (150, 151). Their Fab and Fv fragments can often be produced efficiently in plants (152, 153) or microorganisms (154). Technical advances in microbial fermentation can be expected to make antibody production economically even more favorable in the future.

In short, current levels of activity may be adequate for some laboratory applications, but higher efficiencies would certainly be beneficial. A 10³-fold increase in turnover would mean that 10³-fold less catalyst is needed to achieve useful levels of performance. Enhanced proficiency will certainly be necessary if energetically more demanding reactions are to be tackled. The creation of antibody equivalents of site-specific proteases, glycosidases, and nucleases, for example, remains a significant yet unrealized goal. The use of antibodies to synthesize or modify structurally complex and biologically important macromolecules will depend on solving this basic problem.

Strategies for Optimizing Efficiency

If imperfect design and indirect selection for binding rather than function are the primary reasons for low catalytic efficiency, creation of substantially better antibody catalysts will be feasible. Conceptually, two approaches can be envisaged: (a) refining methods for producing first generation catalysts, and (b) developing new

strategies to optimize existing active sites. Improved transition-state analogs and more effective screening of the immune response address the first point. Rational reengineering and directed evolution methods are relevant to the second. These strategies have already been discussed in the context of specific antibody catalysts but are summarized in more general terms below.

Better Haptens The rewards of good—and the penalties of deficient—design are evident in the properties of catalytic antibodies characterized to date. In general, however, it is not clear which of the structural features of a transition state are most important to mimic to elicit maximally effective catalysts. Statistically meaningful correlation of different hapten types and the properties of their complementary active sites are needed to optimize analogs for each type of reaction.

Incorporating design features that maximize transition-state affinity while minimizing ground state stabilization remains a major challenge (12). For example, aryl groups are constituents of many haptens. Binding energy directed toward them, while increasing hapten affinity, may be useless or even harmful for catalysis, since these elements are common to both ground and transition state. Inefficient use of intrinsic binding energy in this way may help to explain the modest activities seen in the oxy-Cope (38) and Diels-Alder reactions (53) discussed above. The finding that catalytic activity for a series of polyclonal esterases correlates inversely with the size and hydrophobicity of the haptenic aryl phosphates (155) also illustrates this problem. When binding energy is used to recognize parts of the substrate distant from the site of reaction, product inhibition becomes another concern. Strategies to facilitate product release must therefore be considered integral to hapten design. Antigen presentation is a further issue. Small molecules are not immunogenic and must be coupled to carrier proteins. Variation of the tether site may be a useful means of focusing immunorecognition on the catalytically relevant epitopes of a hapten (141).

Linkage of chemical reactivity with the selection and amplification processes of the immune system may mitigate some limitations in design. For this reason, the reactive immunization strategy (19, 118–122) merits increased attention. Many additional examples will be needed to establish its true scope and limitations. Given their importance in natural enzymes (156), metal ions and exogenous organic cofactors should considerably extend the properties of antibody catalysts, as well. Although versatile hybrid catalysts that combine the intrinsic reactivity of the metal ion or coenzyme with the tailored binding specificity of the antibody can be readily envisaged, this strategy has been surprisingly underutilized. Metal ion binding sites have been engineered into antibody binding sites (157), creating a sensitive Zn(II) sensor in one case (158), but catalysis has not been realized. An alternative, seemingly promising strategy using metal chelates for peptide cleavage has received little attention since first reported (159). Modest activities have been described for other miscellaneous cofactor-dependent reactions (158, 160–163), but more work is obviously needed. Such strategies will be very important for promoting reactions with high kinetic barriers and reactions that cannot be carried out with protein residues alone.

Screening Because unusual germ line sequences or fortuitous mutations may be necessary for high activity, the best antibody catalysts are also potentially the rarest. For this reason, more extensive screening of the immune response may substantially increase the probability of finding highly active clones. Usually, small panels of antibodies chosen for their ability to bind the transition-state analog are purified and tested individually for catalytic activity. This procedure is necessarily indirect and slow. Sensitive chemical (164), biological (42, 77, 91, 165), and immunological assays (60, 166, 167) can facilitate the screening of thousands of candidates directly for catalysis and thereby accelerate the preliminary evaluation process.

One practical problem associated with broad screening is that some antigens yield many hapten binders, others relatively few. To increase the size and diversity of the antibody population available for testing, multiple fusions can be performed and several mouse strains used for immunization. Mice prone to autoimmunity have been shown to yield unusually large numbers of esterolytic antibodies and may prove more generally useful for expanding the repertoire of catalytic clones elicited by a single transition-state analog (168).

Significant progress has also been made in copying the combinatorial processes of the immune system *in vitro*. Libraries of antibody fragments containing more than 10^6 members can be constructed and produced in microorganisms or displayed on phage particles (169–172). These systems are attractive vehicles for exploring the catalytic potential of different subsets of the primary immunological repertoire. Binders can be selected from these libraries on the basis of hapten affinity and subsequently screened for catalytic activity (169). Clever strategies for capturing active clones based on their activity should be even more effective (173–177). Alternatively, catalysts can be obtained directly by selection *in vivo* using yeast or bacterial auxotrophs (42, 77, 91). In these approaches, iterative rounds of mutagenesis and reselection replace somatic mutation as a means of refining initial hits (170). Domain swapping (178) and powerful DNA shuffling methods (179, 180) have been developed to speed this process.

Engineering The upper limit on activity that can be achieved with antibodies is unknown and may be reaction dependent. It is therefore important to push several test cases as far as possible. Site-directed mutagenesis is an attractive tool for improving catalytic power, particularly given the availability of increasing numbers of high-resolution structures. In general, it will probably be easiest to reengineer the poorest catalysts, since changes that improve packing or provide missing but critical interactions may be relatively obvious. The mutational study leading to an order of magnitude increase in activity of the Diels-Alderase antibody 39-A11 is a case in point (54). The fact that relatively few changes are needed to tailor the properties of germ line structure during affinity maturation (53, 85, 93) is also encouraging. Pinpointing subtle changes needed to optimize more active clones is likely to be more difficult, however. The obstacles encountered in augmenting the activity of hydrolytic antibodies sound a cautionary note (103–105). Ultimately, our understanding of structure-function relationships will determine what can be achieved in this way.

Selection Enzymes have been brought to peak efficiency over millions of years by the process of natural selection. An analogous process in the laboratory, involving recursive cycles of mutagenesis and genetic selection for function, may provide the ultimate test of the capabilities of antibody catalysts. Evolution of antibodies can be accomplished perhaps most directly by complementation of auxotrophic yeast or bacterial strains. The chorismate mutase antibody 1F7 (42) and an orotate decarboxylase antibody (77) have been shown to confer a significant growth advantage under selective conditions to host cells lacking the corresponding enzymes. Though the experiments are technically difficult because of poor antibody expression in microorganisms, preliminary results with the chorismate mutase antibody have demonstrated the feasibility of selecting antibodies with novel properties (43). Recent work showing that cytoplasmic production of antibody fragments is optimizable by selection (181) augurs well for these efforts. Selection systems are available for many transformations, including the ferrochelatase and metabolic reactions already mentioned (42, 70, 77). A generalized selection scheme for hydrolytic reactions has also been reported (91); analogous assays could be developed to exploit the ability of a catalyst to synthesize or destroy nutrients, drugs, hormones, or toxins. In addition to providing clues about the perfectibility of catalytic antibodies, such experiments may yield fundamental insights into structure-activity relationships and the evolution of molecular function.

Other Scaffolds The immune system was originally tapped as a source of catalysts as a matter of convenience: It is unrivaled in its ability to fashion high-affinity protein receptors—the antibodies—to virtually any natural or synthetic molecule, essentially on demand (58, 136, 137). However, now that the combinatorial processes of the immune system can be mimicked in vitro and libraries of macromolecules generated relatively easily using the tools of molecular biology, there is no compelling need to restrict Jencks' original strategy to a single protein fold or even to a single class of macromolecule.

Indeed, analogous to catalytic antibody experiments, catalytic RNAs and DNAs have been obtained from large libraries of nucleic acids by selection for binding to transition-state analogs. Catalysts for porphyrin metallation obtained in this way (182–184) have activity comparable to that of the ferrochelatase antibody 7G12 discussed above, but an RNA rotamase is 30-fold less effective than its antibody counterpart (185). The lower activity of the latter largely reflects the lower affinity of the RNA for the hapten used ($K_d = 7 \mu\text{M}$, compared with $0.21 \mu\text{M}$ for the antibody). A similar explanation has been invoked for RNAs that bind the 1E9 hapten (compound 4, Figure 6) but fail to catalyze the corresponding Diels-Alder reaction (186). Nucleic acids are likely to be intrinsically more limited than proteins in their capacity for high-affinity molecular recognition of structurally diverse ligands as well as for catalysis (187).

Direct selection for function rather than transition-state analog binding has proved to be a much more powerful approach for obtaining nucleic acids with novel catalytic properties (for a recent comprehensive review, see 188). RNA and

DNA catalysts have been prepared for a variety of reactions, including a Diels-Alder cycloaddition (189), in this way. Although the resulting catalysts often have relatively modest efficiency, phosphoryl transfers, which are difficult to achieve with antibodies because of the dearth of stable analogs of the pentacoordinate transition state, have been particularly amenable to catalysis. One of the most impressive accomplishments in this regard is the selection of highly efficient ribozymes capable of a self-ligation reaction from large pools of random sequence (190). The number of starting molecules in these experiments was huge ($\sim 10^{15}$), dwarfing the diversity of the primary immune repertoire ($\sim 10^8$ molecules), allowing even extremely rare catalysts to be found. One of the ribozymes obtained by selection was subsequently reengineered to function as a true catalyst; it promotes an intermolecular ligation with multiple turnovers and a rate acceleration approaching 10^9 (191). This impressive activity is higher than that of most antibody catalysts, and provides an impressive demonstration of the power of direct selection.

In principle, *in vitro* selection of peptides and proteins from vast combinatorial libraries is now possible as well using ribosome display (192–194), mRNA-protein fusion methods (195, 196), and more established phage display formats (172). Coupled with efficient ways of linking genotype with phenotype (174–176), these methods can be expected to facilitate the production of proteins with novel properties and functions. As such, they powerfully complement other efforts to harness the power of evolution to redesign the structures and activities of existing enzymes (197–199, 207, 208).

CONCLUSIONS

Catalytic antibody technology combines programmable design with the combinatorial diversity of the immune system. This fusion has allowed the field to progress in relatively short order from simple model reactions to complex multistep processes, but much remains to be learned. Early efforts focused largely on defining the scope and limitations of this technology. Now that the approach is well established, attention must be paid to strategies for optimizing catalytic efficiency and for promoting more demanding transformations. In many ways, these are far greater challenges than identifying first-generation catalysts with modest activity. Continued mechanistic and structural analysis of these systems will inform such endeavors. In addition, learning how to create, manipulate, and evolve large combinatorial libraries of proteins outside the immune system should help to automate the processes of catalyst discovery and optimization.

ACKNOWLEDGMENTS

The author is indebted to Kinya Hotta for creating the graphics for this article and to the National Institutes of Health, the ETH Zurich, the Swiss National Science Foundation, and Novartis Pharma for generous support.

Visit the Annual Reviews home page at www.AnnualReviews.org

LITERATURE CITED

1. Jencks WP. 1969. *Catalysis in Chemistry and Enzymology*. New York: McGraw-Hill
2. Schultz PG, Lerner RA. 1995. *Science* 269:1835–42
3. Hilvert D. 1999. In *Topics in Stereochemistry*, ed. SE Denmark, 22:83–135. New York: Wiley
4. Schultz PG, Lerner RA. 1993. *Acc. Chem. Res.* 26:391–95
5. Sinha SC, Barbas CF III, Lerner RA. 1998. *Proc. Natl. Acad. Sci. USA* 95:14603–8
6. Shabat D, Rader C, List B, Lerner RA, Barbas CF III. 1999. *Proc. Natl. Acad. Sci. USA* 96:6925–30
7. Radzicka A, Wolfenden R. 1995. *Science* 267:90–93
8. Wolfenden R, Lu XD, Young G. 1998. *J. Am. Chem. Soc.* 120:6814–15
9. Pauling L. 1948. *Am. Sci.* 36:51–58
10. Kurz JL. 1963. *J. Am. Chem. Soc.* 85:987–91
11. Wolfenden R. 1969. *Nature* 223:704–5
12. Mader MM, Bartlett PA. 1997. *Chem. Rev.* 97:1281–1301
13. Radzicka A, Wolfenden R. 1995. *Methods Enzymol.* 249:284–303
14. Lolis E, Petsko GA. 1990. *Annu. Rev. Biochem.* 59:597–630
15. Stewart JD, Benkovic SJ. 1995. *Nature* 375:388–91
16. Thomas NR. 1994. *Appl. Biochem. Biotechnol.* 47:345–72
17. Abeles RH, Maycock AL. 1976. *Acc. Chem. Res.* 9:313–19
18. Walsh C. 1982. *Tetrahedron* 38:871–909
19. Wirsching P, Ashley JA, Lo C-HL, Janda KD, Lerner RA. 1995. *Science* 270:1775–82
20. Jencks WP. 1975. *Adv. Enzymol.* 43:219–410
21. Westheimer FH. 1962. *Adv. Enzymol.* 24:441–82
22. Bartlett PA, Nakagawa Y, Johnson CR, Reich SH, Luis A. 1988. *J. Org. Chem.* 53:3195–210
23. Gray JV, Eren D, Knowles JR. 1990. *Biochemistry* 29:8872–78
24. Hilvert D, Nared KD. 1988. *J. Am. Chem. Soc.* 110:5593–94
25. Hilvert D, Carpenter SH, Nared KD, Auditor M-TM. 1988. *Proc. Natl. Acad. Sci. USA* 85:4953–55
26. Jackson DY, Jacobs JW, Sugasawara R, Reich SH, Bartlett PA, Schultz PG. 1988. *J. Am. Chem. Soc.* 110:4841–42
27. Jackson DY, Liang MN, Bartlett PA, Schultz PG. 1992. *Angew. Chem. Int. Ed. Engl.* 31:182–83
28. Lee AY, Stewart JD, Clardy J, Ganem B. 1995. *Chem. Biol.* 2:195–203
29. Campbell PA, Tarasow TM, Masefski W, Wright PE, Hilvert D. 1993. *Proc. Natl. Acad. Sci. USA* 90:8663–67
30. Haynes MR, Stura EA, Hilvert D, Wilson IA. 1994. *Science* 263:646–52
31. Addadi L, Jaffe EK, Knowles JR. 1983. *Biochemistry* 22:4494–501
32. Gustin DJ, Mattei P, Kast P, Wiest O, Lee L, et al. 1999. *J. Am. Chem. Soc.* 121:1756–57
33. Kast P, Asif-Ullah M, Jiang N, Hilvert D. 1996. *Proc. Natl. Acad. Sci. USA* 93:5043–48
34. Liu DR, Cload ST, Pastor RM, Schultz PG. 1996. *J. Am. Chem. Soc.* 118:1789–90
35. Wiest O, Houk KN. 1994. *J. Org. Chem.* 59:7582–84
36. Braisted AC, Schultz PG. 1994. *J. Am. Chem. Soc.* 116:2211–12
37. Driggers EM, Cho HS, Liu CW, Katzka CW, Braisted AC, et al. 1998. *J. Am. Chem. Soc.* 120:1945–58
38. Ulrich HD, Mundorff E, Santarsiero BD, Driggers EM, Stevens RC, Schultz PG. 1997. *Nature* 389:271–75
39. Görisch J. 1978. *Biochemistry* 17:3700–5

40. Kast P, Asif-Ullah M, Hilvert D. 1996. *Tetrahedron Lett.* 37:2691–94
41. Steigerwald MJ, Goddard WA, Evans DA. 1979. *J. Am. Chem. Soc.* 101:1994–97
42. Tang Y, Hicks JB, Hilvert D. 1991. *Proc. Natl. Acad. Sci. USA* 88:8784–86
43. Tang Y. 1996. *Evolutionary studies with a catalytic antibody*. PhD thesis. The Scripps Res. Inst., La Jolla, CA. 143 pp.
44. Sauer J, Sustman R. 1980. *Angew. Chem. Int. Ed. Engl.* 19:779–807
45. Hilvert D, Hill KW, Nared KD, Auditor M-TM. 1989. *J. Am. Chem. Soc.* 111:9261–62
46. Gouverneur VE, Houk KN, Pascual-Teresa B, Beno B, Janda KD, Lerner RA. 1993. *Science* 262:204–8
47. Braisted AC, Schultz PG. 1990. *J. Am. Chem. Soc.* 112:7430–31
48. Yli-Kauhaluoma JT, Ashley JA, Lo C-H, Tucker L, Wolfe MM, Janda KD. 1995. *J. Am. Chem. Soc.* 117:7041–47
49. Resmini M, Meekel AAP, Pandit UK. 1996. *Pure Appl. Chem.* 68:2025–28
50. Kirby AJ. 1980. *Adv. Phys. Org. Chem.* 17:183–278
51. Page MI, Jencks WP. 1971. *Proc. Natl. Acad. Sci. USA* 68:1678–83
52. Xu J, Deng Q, Chen J, Houk KN, Bartek J, Hilvert D, Wilson IA. 1999. *Science* 286:2345–48
53. Romesberg FE, Spiller B, Schultz PG, Stevens RC. 1998. *Science* 279:1929–33
54. Romesberg FE, Schultz PG. 1999. *Bioorg. Med. Chem. Lett.* 9:1741–44
55. Haynes MR, Lenz M, Taussig MJ, Wilson IA, Hilvert D. 1996. *Isr. J. Chem.* 36:151–59
56. Arevalo JH, Taussig MJ, Wilson IA. 1993. *Nature* 365:859–63
57. Arevalo JH, Hassig CA, Stura EA, Sims MJ, Taussig MJ, Wilson IA. 1994. *J. Mol. Biol.* 241:663–90
58. Kabat EA. 1976. *Structural Concepts in Immunology and Immunochemistry*. New York: Holt, Rinehart, & Winston
59. Laschat S. 1996. *Angew. Chem. Int. Ed. Engl.* 35:289–91
60. MacBeath G, Hilvert D. 1994. *J. Am. Chem. Soc.* 116:6101–6
61. Haldane JBS. 1930. *Enzymes*. London: Longmans, Green
62. Lavalee DK. 1988. *Mol. Struct. Energ.* 9: 279–314
63. Al-Karadaghi S, Hansson M, Nikonov S, Jonsson B, Hederstedt L. 1997. *Structure* 5:1501–10
64. Dailey HA, Fleming JE. 1983. *J. Biol. Chem.* 258:11453–59
65. Cochran AG, Schultz PG. 1990. *Science* 249:781–83
66. Hansson M, Hederstedt L. 1994. *Eur. J. Biochem.* 220:201–8
67. Romesberg FE, Santarsiero BD, Spiller B, Yin J, Barnes D, et al. 1998. *Biochemistry* 37:14404–9
68. Blackwood ME Jr, Rush TS III, Romesberg F, Schultz PG, Spiro TG. 1998. *Biochemistry* 37:779–82
69. Warshel A. 1998. *J. Biol. Chem.* 273: 27035–38
70. Gora M, Grzybowska E, Rytka J, Labbe-Bois R. 1996. *J. Biol. Chem.* 271:11810–16
71. Crosby J, Stone R, Lienhard GE. 1970. *J. Am. Chem. Soc.* 92:2891–900
72. O’Leary MH, Piazza GJ. 1981. *Biochemistry* 20:2743–48
73. Alston TA, Abeles RH. 1987. *Biochemistry* 26:4082–85
74. Sun SX, Duggleby RG, Schowen RL. 1995. *J. Am. Chem. Soc.* 117:7317–22
75. Lewis C, Krämer T, Robinson S, Hilvert D. 1991. *Science* 253:1019–22
76. Tarasow TM, Lewis C, Hilvert D. 1994. *J. Am. Chem. Soc.* 116:7959–63
77. Smiley JA, Benkovic SJ. 1994. *Proc. Natl. Acad. Sci. USA* 91:8319–23
78. Bartlett PA, Marlow CK. 1983. *Biochemistry* 22:4618–24
79. Stewart JD, Liotta LJ, Benkovic SJ. 1993. *Acc. Chem. Res.* 26:396–404
80. Charbonnier J-B, Carpenter E, Gigant B, Golinelli-Pimpaneau B, Tawfik D, et al.

1995. *Proc. Natl. Acad. Sci. USA* 92: 11721–25
81. Golinelli-Pimpaneau B, Gigant B, Bizebard T, Navaza J, Saludjian P, et al. 1994. *Structure* 2:175–83
82. Kristensen O, Vassilyev DG, Tanaka F, Morikawa K, Fujii I. 1998. *J. Mol. Biol.* 281:501–11
83. Charbonnier J-B, Golinelli-Pimpaneau B, Gigant B, Tawfik DS, Chap R, et al. 1997. *Science* 275:1140–42
84. Gigant B, Charbonnier J-B, Eshhar Z, Green BS, Knossow M. 1997. *Proc. Natl. Acad. Sci. USA* 94:7857–61
85. Patten PA, Gray NS, Yang PL, Marks CB, Wedemayer GJ, et al. 1996. *Science* 271:1086–90
86. Wedemayer GJ, Wang LH, Patten PA, Schultz PG, Stevens RC. 1997. *J. Mol. Biol.* 268:390–400
87. Wedemayer GJ, Patten PA, Wang LH, Schultz PG, Stevens RC. 1997. *Science* 276:1665–69
88. Thayer MM, Olender EH, Arvai AS, Koike CK, Canestrelli IL, et al. 1999. *J. Mol. Biol.* 291:329–45
89. Zhou GW, Guo J, Huang W, Fletterick RJ, Scanlan TS. 1994. *Science* 265:1059–64
90. Guo J, Huang W, Zhou GW, Fletterick RJ, Scanlan TS. 1995. *Proc. Natl. Acad. Sci. USA* 92:1694–98
91. Lesley SA, Patten PA, Schultz PG. 1993. *Proc. Natl. Acad. Sci. USA* 90:1160–65
92. Lindner AB, Eshhar Z, Tawfik DS. 1998. *J. Mol. Biol.* 285:421–30
93. Tomlinson IM, Walter G, Jones PT, Dear PH, Sonhammer ELL, Winter G. 1996. *J. Mol. Biol.* 256:813–17
94. Wells JA, Cunningham BC, Graycar TP, Estell DA. 1986. *Philos. Trans. R. Soc. London Ser. A* 317:415–23
95. Bryan P, Pantoliano MW, Quill SG, Hsiao H-Y, Poulos T. 1986. *Proc. Natl. Acad. Sci. USA* 83:3743–45
96. MacBeath G, Hilvert D. 1996. *Chem. Biol.* 3:433–45
97. Padlan EA, Cohen GH, Davies DR. 1985. *Ann. Inst. Pasteur Immunol.* 136C:271–76
98. Strong RK, Petsko GA, Sharon J, Margolies MN. 1991. *Biochemistry* 30:3749–57
99. Griffiths GM, Berek C, Kaartinen M, Milstein C. 1984. *Nature* 312:271–75
100. Alzari PM, Spinelli S, Mariuzza RA, Boulot G, Poljak RJ, et al. 1990. *EMBO J.* 9:3807–14
101. Miyashita H, Karaki Y, Kikuchi M, Fujii I. 1993. *Proc. Natl. Acad. Sci. USA* 90:5337–40
102. Roberts VA, Stewart J, Benkovic SJ, Getzoff ED. 1994. *J. Mol. Biol.* 235:1098–116
103. Stewart JD, Roberts VA, Thomas NR, Getzoff ED, Benkovic SJ. 1994. *Biochemistry* 33:1994–2003
104. Baca M, Scanlan TS, Stephenson RC, Wells JA. 1997. *Proc. Natl. Acad. Sci. USA* 94:10063–68
105. Arkin MR, Wells JA. 1998. *J. Mol. Biol.* 284:1083–94
106. Janda KD, Benkovic SJ, Lerner RA. 1989. *Science* 244:437–40
107. Benkovic SJ, Adams JA, Borders CL, Janda KD, Lerner RA. 1990. *Science* 250:1135–39
108. Fernholz E, Schloeder D, Liu KK-C, Bradshaw CW, Huang H, et al. 1991. *J. Org. Chem.* 57:4756–61
109. Stewart JD, Krebs JF, Siuzdak G, Berdis AJ, Smithrud DB, Benkovic SJ. 1994. *Proc. Natl. Acad. Sci. USA* 91:7404–9
110. Janda KD, Schloeder D, Benkovic SJ, Lerner RA. 1988. *Science* 241:1188–91
111. Krebs JF, Siuzdak G, Dyson J. 1995. *Biochemistry* 34:720–23
112. Carter P, Wells JA. 1988. *Nature* 332:564–68
113. Gibbs RA, Benkovic PA, Janda KD, Lerner RA, Benkovic SJ. 1992. *J. Am. Chem. Soc.* 114:3528–34
114. Lerner RA, Benkovic SJ, Schultz PG. 1991. *Science* 252:659–67

115. Thorn SN, Daniels RG, Auditor M-TM, Hilvert D. 1995. *Nature* 373:228–30
116. Suga H, Ersoy O, Williams SF, Tsumuraya T, Margolies MN, et al. 1994. *J. Am. Chem. Soc.* 116:6025–26
117. Tsumuraya T, Suga H, Meguro S, Tsunakawa A, Masamune S. 1995. *J. Am. Chem. Soc.* 117:11390–96
118. Janda K, Lo C-H, Li T, Barbas CF, Wirsching P, Lerner RA. 1994. *Proc. Natl. Acad. Sci. USA* 91:2532–36
119. Janda KD, Lo L-C, Lo C-HL, Sim M-M, Wang R, et al. 1997. *Science* 275:945–48
120. Wagner J, Lerner R, Barbas C. 1995. *Science* 270:1797–800
121. Lo C-HL, Wentworth P Jr, Jung KW, Yoon J, Ashley JA, Janda KD. 1997. *J. Am. Chem. Soc.* 119:10251–52
122. Gao C, Lavey BJ, Lo C-HL, Datta A, Wentworth P Jr, Janda KD. 1998. *J. Am. Chem. Soc.* 120:2211–17
123. Barbas CF III, Heine A, Zhong G, Hoffmann T, Gramatikova S, et al. 1997. *Science* 278:2085–92
124. Horecker BL, Tsolas O, Lai C-Y. 1975. In *The Enzymes*, ed. PD Boyer, 7:213–58. New York: Academic
125. Marsh JJ, Lebherz HG. 1992. *Trends Biochem. Sci.* 17:110–13
126. Highbarger LA, Gerlt JA, Kenyon GL. 1996. *Biochemistry* 35:41–46
127. Hoffmann T, Zhong G, List B, Shabat D, Anderson J, et al. 1998. *J. Am. Chem. Soc.* 120:2768–79
128. Zhong G, Hoffmann T, Lerner RA, Danishefsky S, Barbas CF III. 1997. *J. Am. Chem. Soc.* 119:8131–32
129. List B, Shabat D, Zhong G, Turner JM, Li A, et al. 1999. *J. Am. Chem. Soc.* 121:7283–91
130. List B, Shabat D, Barbas CF III, Lerner RA. 1998. *Chem. Eur. J.* 4:881–85
131. Penttoet EE, Kochman M, Rutter WJ. 1969. *Biochemistry* 8:4396–402
132. Hammerstedt RH, Möhler H, Decker KA, Ersfeld DE, Wood WA. 1975. *Methods Enzymol.* 42C:258–64
133. Branden C, Tooze J. 1991. *Introduction to Protein Structure*. New York: Garland
134. Wilson IA, Stanfield RL. 1993. *Curr. Opin. Struct. Biol.* 3:113–18
135. Davies DR, Padlan EA, Sheriff S. 1990. *Annu. Rev. Biochem.* 59:439–73
136. Alt FW, Blackwell TK, Yancopoulos GD. 1987. *Science* 238:1079–87
137. Rajewsky K, Förster I, Cumang A. 1987. *Science* 238:1088–94
138. Tsou CL. 1998. *Ann. NY Acad. Sci.* 864: 1–8
139. Post CB, Ray WJ Jr. 1995. *Biochemistry* 34:15881–85
140. Mets B, Winger G, Cabrera C, Seo S, Jamdar S, et al. 1998. *Proc. Natl. Acad. Sci. USA* 95:10176–81
141. Yang G, Chun J, Arakawa-Uramoto H, Wang X, Gawinowicz MA, et al. 1996. *J. Am. Chem. Soc.* 118:5881–90
142. Cravatt BF, Ashley JA, Janda KD, Boger DL, Lerner RA. 1994. *J. Am. Chem. Soc.* 116:6013–14
143. Janda KD, Shevlin CG, Lerner RA. 1993. *Science* 259:490–93
144. Janda KD, Shevlin CG, Lerner RA. 1995. *J. Am. Chem. Soc.* 117:2659–60
145. Shabat D, Itzhaky H, Reymond J-L, Keinan E. 1995. *Nature* 374:143–46
146. Li T, Janda KD, Lerner RA. 1996. *Nature* 379:326–27
147. Reymond J-L, Reber J-L, Lerner RA. 1994. *Angew. Chem. Int. Ed. Engl.* 33: 475–77
148. Sinha SC, Keinan E. 1995. *J. Am. Chem. Soc.* 117:3653–54
149. Harlow E, Lane D. 1988. *Antibodies: A Laboratory Manual*. Cold Spring Harbor, NY: Cold Spring Harbor Lab. Press
150. Lowry D, Murphy S, Goffe RA. 1994. *J. Biotechnol.* 36:35–38
151. Jackson LR, Trudel LJ, Fox JG, Lipman NS. 1996. *J. Immunol. Methods* 189:217–31
152. Ma JKC, Hiatt A, Hein M, Vine ND, Wang F, et al. 1995. *Science* 268:716–19

153. Hiatt A, Ma JKC. 1992. *FEBS Lett.* 307: 71–75
154. Carter P, Kelley RF, Rodrigues ML, Snedecor B, Covarrubias M, et al. 1992. *Bio/Technology* 10:163–67
155. Wallace MB, Iverson BL. 1996. *J. Am. Chem. Soc.* 118:251–52
156. Walsh C. 1979. *Enzymatic Reaction Mechanisms*. New York: Freeman
157. Iverson BL, Iverson SA, Roberts VA, Getzoff ED, Tainer JA, et al. 1990. *Science* 249:659–62
158. Stewart JD, Roberts VA, Crowder MW, Getzoff ED, Benkovic SJ. 1994. *J. Am. Chem. Soc.* 116:415–16
159. Iverson BL, Lerner RA. 1989. *Science* 243:1184–88
160. Shokat KM, Leumann CJ, Sugawara R, Schultz PG. 1988. *Angew. Chem. Int. Ed. Engl.* 27:1172–74
161. Nimri S, Keinan E. 1999. *J. Am. Chem. Soc.* 121:8978–82
162. Cochran AG, Schultz PG. 1990. *J. Am. Chem. Soc.* 112:9414–15
163. Cochran AG, Pham T, Sugawara R, Schultz PG. 1991. *J. Am. Chem. Soc.* 113: 6670–72
164. Eisenthal R, Danson MJ. 1993. *Enzyme Assays—A Practical Approach*. Oxford, UK: IRL
165. Fenniri H, Janda KD, Lerner RA. 1995. *Proc. Natl. Acad. Sci. USA* 92:2278–82
166. Lee I, Stewart JD, Zhong W, Benkovic SJ. 1995. *Anal. Biochem.* 230:62–67
167. Tawfik DS, Green BS, Chap R, Sela M, Eshhar Z. 1993. *Proc. Natl. Acad. Sci. USA* 90:373–77
168. Tawfik DS, Chap R, Green BS, Sela M, Eshhar Z. 1995. *Proc. Natl. Acad. Sci. USA* 92:2145–49
169. Chiswell DJ, McCafferty J. 1992. *Trends Biotechnol.* 10:80–84
170. Marks JD, Hoogenboom HR, Griffiths AD, Winter G. 1992. *J. Biol. Chem.* 267: 16007–10
171. Huse WD, Sastry L, Iverson SA, Kang AS, Alting-Mees M, et al. 1989. *Science* 246:1275–81
172. Smith GP, Petrenko VA. 1997. *Chem. Rev.* 97:391–410
173. Jestin JL, Kristensen P, Winter G. 1999. *Angew. Chem. Int. Ed. Engl.* 38:1224–27
174. Gao C, Lin CH, Lo C-HL, Mao S, Wirsching P, et al. 1997. *Proc. Natl. Acad. Sci. USA* 94:11777–82
175. Pedersen H, Holder S, Sutherlin DP, Schwitter U, King DS, Schultz PG. 1998. *Proc. Natl. Acad. Sci. USA* 95:10523–28
176. Tawfik DS, Griffiths AD. 1998. *Nat. Biotechnol.* 16:652–56
177. Soumillion P, Jespers L, Bouchet M, Marchand-Brynaert J, Winter G, Fastrez J. 1994. *J. Mol. Biol.* 237:415–22
178. Miller GP, Posner BA, Benkovic SJ. 1997. *Bioorg. Med. Chem.* 5:581–90
179. Stemmer WPC. 1994. *Nature* 370:389–91
180. Cramer A, Cwirla S, Stemmer WPC. 1996. *Nat. Med.* 2:100–2
181. Martineau P, Jones P, Winter G. 1998. *J. Mol. Biol.* 280:117–27
182. Conn MM, Prudent JR, Schultz PG. 1996. *J. Am. Chem. Soc.* 118:7012–13
183. Li Y, Sen D. 1996. *Nat. Struct. Biol.* 3:743–47
184. Li Y, Sen D. 1997. *Biochemistry* 36: 5589–99
185. Prudent JR, Uno T, Schultz PG. 1994. *Science* 264:1924–27
186. Morris KN, Tarasow TM, Julin CM, Simons S, Hilvert D, Gold L. 1994. *Proc. Natl. Acad. Sci. USA* 91:13028–32
187. Narlikar GJ, Herschlag D. 1997. *Annu. Rev. Biochem.* 66:19–59
188. Wilson DS, Szostak JW. 1999. *Annu. Rev. Biochem.* 68:611–47
189. Tarasow TM, Tarasow SL, Eaton BE. 1997. *Nature* 389:54–57
190. Bartel DP, Szostak JW. 1993. *Science* 261:1411–18
191. Eklund EH, Szostak JW, Bartel DP. 1995. *Science* 269:364–70

192. Hanes J, Plückthun A. 1997. *Proc. Natl. Acad. Sci. USA* 94:4937–42
193. Hanes J, Jermutus L, Weber-Bornhauser S, Bosshard HR, Plückthun A. 1998. *Proc. Natl. Acad. Sci. USA* 95:14130–35
194. He M, Taussig MJ. 1997. *Nucleic Acids Res.* 25:5132–34
195. Roberts RW, Szostak JW. 1997. *Proc. Natl. Acad. Sci. USA* 94:12297–302
196. Nemoto N, Miyamoto-Sato E, Husimi Y, Yanagawa H. 1997. *FEBS Lett.* 414:405–8
197. MacBeath G, Kast P, Hilvert D. 1998. *Science* 279:1958–61
198. Minshull J, Stemmer WPC. 1999. *Curr. Opin. Chem. Biol.* 3:284–90
199. Arnold FH. 1998. *Acc. Chem. Res.* 31:125–31
200. Shokat KM, Leumann CJ, Sugasawara R, Schultz PG. 1989. *Nature* 338:269–71
201. Tawfik DS, Lindner AB, Chap R, Eshhar Z, Green BS. 1997. *Eur. J. Biochem.* 244:619–26
202. Zemel R, Schindler DG, Tawfik DS, Eshhar Z, Green BS. 1994. *Mol. Immunol.* 31:127–37
203. Lee AY, Karplus AP, Ganem B, Clardy J. 1995. *J. Am. Chem. Soc.* 117:3627–28
204. Esnouf RM. 1997. *J. Mol. Graph. Model.* 15:132–34
205. Merritt EA, Murphy MEP. 1994. *Acta Crystallogr.* D50:869–73
206. Nicholls A, Sharp KA, Honig B. 1991. *Proteins: Struct. Funct. Genet.* 11:281–96
207. Joo H, Lin ZL, Arnold FH. 1999. *Nature* 399:670–73
208. Altamirano MM, Blackburn JM, Aguayo C, Fersht AR. 2000. *Nature* 403:617–22



CONTENTS

STILL LOOKING FOR THE IVORY TOWER, <i>Howard K. Schachman</i>	1
CRYPTOCHROME: The Second Photoactive Pigment in The Eye and Its Role in Circadian Photoreception, <i>Aziz Sançar</i>	31
PROTEIN GLUCOSYLATION AND ITS ROLE IN PROTEIN FOLDING, <i>Armando J. Parodi</i>	69
SPINDLE ASSEMBLY IN ANIMAL CELLS, <i>Duane A. Compton</i>	95
CHROMOSOME COHESION, CONDENSATION, AND SEPARATION, <i>Tatsuya Hirano</i>	115
CYCLOOXYGENASES: Structural, Cellular, and Molecular Biology, <i>William L. Smith, David L. DeWitt, and R. Michael Garavito</i>	145
TWO-COMPONENT SIGNAL TRANSDUCTION, <i>Ann M. Stock, Victoria L. Robinson, and Paul N. Goudreau</i>	183
APOPTOSIS SIGNALING, <i>Andreas Strasser, Liam O'Connor, and Vishva M. Dixit</i>	217
YEAST HOMOTYPIC VACUOLE FUSION: A Window on Organelle Trafficking Mechanisms, <i>William Wickner and Albert Haas</i>	247
STRUCTURAL INSIGHTS INTO MICROTUBULE FUNCTION, <i>Eva Nogales</i>	277
AUTOPHAGY, CYTOPLASM-TO-VACUOLE TARGETING PATHWAY, AND PEXOPHAGY IN YEAST AND MAMMALIAN CELLS, <i>John Kim and Daniel J. Klionsky</i>	303
COUPLING OF OPEN READING FRAMES BY TRANSLATIONAL BYPASSING, <i>Alan J. Herr, John F. Atkins, and Raymond F. Gesteland</i>	343
PROTEIN TYROSINE KINASE STRUCTURE AND FUNCTION, <i>Stevan R. Hubbard and Jeffrey H. Till</i>	373
IMPORT OF PEROXISOMAL MATRIX AND MEMBRANE PROTEINS, <i>S. Subramani, Antonius Koller, and William B. Snyder</i>	399
PLATELET-ACTIVATING FACTOR AND RELATED LIPID MEDIATORS, <i>Stephen M. Prescott, Guy A. Zimmerman, Diana M. Stafforini, and Thomas M. McIntyre</i>	419
PROTEIN SPLICING AND RELATED FORMS OF PROTEIN AUTOPROCESSING, <i>Henry Paulus</i>	447
DNA REPLICATION FIDELITY, <i>Thomas A. Kunkel and Katarzyna Bebenek</i>	497
RECEPTOR BINDING AND MEMBRANE FUSION IN VIRUS ENTRY: The Influenza Hemagglutinin, <i>John J. Skehel and Don C. Wiley</i>	531

MECHANISMS AND CONTROL OF MRNA DECAPPING IN <i>Saccharomyces cerevisiae</i> , <i>Morgan Tucker and Roy Parker</i>	571
RIBOZYME STRUCTURES AND MECHANISMS, <i>Elizabeth A. Doherty and Jennifer A. Doudna</i>	597
AMINOACYL-TRNA SYNTHESIS, <i>Michael Ibba and Dieter Söll</i>	617
STRUCTURE AND FUNCTION OF HEXAMERIC HELICASES, <i>S. S. Patel and K. M. Picha</i>	651
CLATHRIN, <i>Tomas Kirchhausen</i>	699
MEDIATOR OF TRANSCRIPTIONAL REGULATION, <i>Lawrence C. Myers and Roger D. Kornberg</i>	729
CRITICAL ANALYSIS OF ANTIBODY CATALYSIS, <i>Donald Hilvert</i>	751
GTPASE-ACTIVATING PROTEINS FOR HETEROTRIMERIC G PROTEINS: Regulators of G Protein Signaling (RGS) and RGS-Like Proteins, <i>Elliott M. Ross and Thomas M. Wilkie</i>	795
REGULATION OF CHROMOSOME REPLICATION, <i>Thomas J. Kelly and Grant W. Brown</i>	829
HELICAL MEMBRANE PROTEIN FOLDING, STABILITY, AND EVOLUTION, <i>Jean-Luc Popot and Donald M. Engelman</i>	881
SYNTHESIS OF NATIVE PROTEINS BY CHEMICAL LIGATION, <i>Philip E. Dawson and Stephen B. H. Kent</i>	923
SWINGING ARMS AND SWINGING DOMAINS IN MULTIFUNCTIONAL ENZYMES: Catalytic Machines for Multistep Reactions, <i>Richard N. Perham</i>	961
STRUCTURE AND FUNCTION OF CYTOCHROME bc COMPLEXES, <i>Edward A. Berry, Mariana Guergova-Kuras, Li-shar Huang, and Antony R. Crofts</i>	1005